EPA-650/2-73-040

December 1973

Environmental Protection Technology Series

DEVELOPMENT OF RANGE SQUARED AND OFF-GATING MODIFICATIONS FOR A LIDAR SYSTEM

Office of Research and Development
U.S. Environmental Protection Agency
Washington, D.C. 20460

EPA-650/2-73-040

DEVELOPMENT OF RANGE SQUARED AND OFF-GATING MODIFICATIONS FOR A LIDAR SYSTEM

by

George W. Bethke

General Electric Company
Space Sciences Laboratory
P. O. Box 8555
Philadelphia, Pa. 19101

Contract No. 68-02-0570
Program Element No. 1A1010

EPA Project Officer. William D. Conner

Chemistry and Physics Laboratory
National Environmental Research Center
Research Triangle Park, N. C. 27711

Prepared for

OFFICE OF RESEARCH AND DEVELOPMENT
U.S. ENVIRONMENTAL PROTECTION AGENCY
WASHINGTON, D. C. 20460

December 1973

This report has been reviewed by the Environmental Protection Agency and approved for publication. Approval does not signify that the contents necessarily reflect the views and policies of the Agency, nor does mention of trade names or commercial products constitute endorsement or recommendation for use.

ABSTRACT

This study was intended to eliminate the dominant source of error in the remote measurement of smoke-stack plumes using lidar, and to improve the data presentation of the lidar transmittance measurement.

The use of a special grid-controlled photomultiplier tube and off-gating system has resulted in a large reduction of photomultiplier tube afterpulsing which has been the principal problem limiting the accuracy of plume transmittance measurements.

A range-correcting time-squared amplifier has also been developed which permits much faster and more convenient data reduction than formerly possible.

The above two developments have been adapted to the existing van-mounted EPA lidar system; and the overall system accuracy has been evaluated using both opaque and semi-transparent targets of known transmittance (T). These test results show the lidar system to yield lidar transmittances (T_L) which (a) are precise to $\pm$ 0.015 average, (b) are accurate to $\pm$ 0.02 average for $T > 0.5$, and (c) are too large at $T < 0.5$ (for example, now $T_L = 0.52$ at $T = 0.50$, and $T_L = 0.28$ at $T = 0.20$). These results are to be compared with the pre-modification accuracies of + .09, -0 at $T > 0.50$, and more severely too large at $T < 0.5$ (for example, formerly $T_L = 0.59$ at $T = 0.50$, and $T_L = 0.40$ at $T = 0.20$).

TABLE OF CONTENTS

TABLE OF CONTENTS (continued)

1. INTRODUCTION

1.1 Background

A mobile lidar (light detection and ranging) system has previously been developed [1,2] for the remote measurement of the transmittance of smoke-stack plumes. A standard pulsed lidar is used for the measurement where atmospheric backscatter of the outgoing pulse is observed as a function of distance. The transmittance of a plume is determined by firing the laser pulse through the plume and measuring the discontinuity between the atmospheric backscatter of the pulse just in front of and behind the plume. Extensive testing of the system [1,2] has shown that the accuracy of the measurement is affected by the intense pulse backscattered by the plume and that data reduction is complicated by the inverse square range dependence of the signal return. Off-gating the photomultiplier detector of the lidar receiver when the backscatter from the plume is received has improved but not eliminated the error. This project is designed to eliminate the lidar error in measuring plume transmittance due to plume backscatter of the laser radiation and to linearize the backscattered signal display with respect to range.

1.2 Purpose of the Program

The study was designed (1) to eliminate the dominant source of error in the remote measurement of the transmittance of smoke-stack plumes using lidar, and (2) to improve the data presentation of the lidar transmittance measurement.

1.3 Scope of Work

The following tasks were to be performed:

1. Develop a time-squared amplifier to range correct the lidar output.
2. Investigate the use of a specially designed grid controlled photomultiplier tube and associated external circuitry to eliminate photomultiplier after-pulsing which results from smoke plume lidar returns.
3. Adapt the time squared amplifier (#1 above) and the grid controlled photomultiplier tube (#2 above) to the existing EPA lidar system.
4. Evaluate the accuracy of the modified system for remote measurement of the transmittance of semi-transparent targets of known transmittance.

2. TECHNICAL BACKGROUND

2.1 The Lidar Concept

The conventional single ended lidar configuration involves a laser transmitter sending out a short pulse of light (10 - 50 nanoseconds) from a laser source in conjunction with a receiving system mounted on a parallel or nearly parallel optical axis which collects backscattered light from the outgoing laser pulse as it propagates away from the system. This collected light is focused on a field-limiting aperture and is then collimated before passing through a narrow band interference filter to a photo-multiplier detector. Thus, backscattered light intensity at the receiving aperture is linearly transformed to voltage across the photomultiplier load resistor as a function of time, and thus range.

When the lidar optical path is through the clear atmosphere, the backscattered signal at the laser wavelength is made up of two components. These are the component due to molecular (Rayleigh) scattering and that due to aerosol (Mie) scattering. A complete expression for system output voltage as a function of range is shown as equation 15 in appendix A of reference 1. However, this expression can be simplified somewhat when considering the relatively short slant ranges at which the plume opacity lidar obtains data. For these ranges, attenuation of the beam and atmospheric density changes can be neglected, with the correct expression for system output voltage being

$$V = \frac{c A S E_o E R}{2 r^2} \left[n(r) \cdot \sigma_R(180^o) + m(r) \cdot \sigma_M(180^o) \right]. \qquad (2.1)$$

where

$$r = ct/2. \qquad (2.2)$$

Here c is the velocity of light, A is the area of the receiving aperture, S is the photomultiplier sensitivity (amps/watt), E_o is the overall system optical efficiency, E is the laser output energy, R is the load resistance, r is the range, n(r) is the number density of molecular scatterers, σ_R (180°) is the Rayleigh backscattering cross section for air, m(r) is the mass concentration of aerosols (μgm/m^3), σ_M(180°) is the mass normalized aerosol (Mie) backscattering cross section, and t is the time since lidar time zero.

If n(r) and m(r) are constant with range then the bracketed term of equation (2.1) is a constant atmospheric backscattering coefficient, k_s, and equations (2.1 and 2.2) become

$$V = 2 A S E_o E R k_s/(ct^2), \qquad (2.3)$$

indicating a basic $1/t^2$ dependence of the system signal.

2.2 Measurement of Plume Transmittance by Lidar

The basic technique used by the EPA lidar system for obtaining the one-way plume transmittance T_L is illustrated in Figure 2.1 which shows a drawing of a lidar return with photomultiplier tube signal voltage plotted against time and thus range. Although the signal voltage is inherently negative, it is shown inverted for clarity in this drawing. The laser pulse is initiated in the transmitter and defines t = 0 for the system. The initiation of this pulse is monitored by a photodiode looking at the laser cavity providing a triggering signal for the system electronics. Since the transmitting and receiving system axes are parallel but not coincident and since the receiving system has a narrow field of view, the backscattered light from the outgoing laser pulse cannot be seen by the receiving system for the first 50 meters or so of range. Following this, the angular field of view of the receiving system combined with the collimated divergence of the laser pulse allows gradual overlap of the two beams with full overlap occurring at a range of approximately 130 meters (0.8 μ sec.). From this point onward the signal return shows a general $1/t^2$ dependence as shown by equation (2.3) as long as the atmospheric scattering coefficient, k_s, is a constant.

Of course a smoke plume means a discontinuous change in k_s which shows up as a sharp signal spike at the range of the plume as indicated in Figure 2.1. The amplitude of this spike can be up to 40 db above the ambient light scattering for low transmittance highly reflecting plumes. Light scattered to the receiver from ranges greater than the plume will have been attenuated by the plume twice, once going out and once coming back. Therefore, the received signal shows a discontinuity at the range of the plume. If the ambient air scattering signal from each side of the plume is extrapolated to a common point in a $1/t^2$ fashion, as shown by the dotted lines in Figure 2.1, the ratio of the two signal levels can be computed as A/B as shown. The one way lidar-determined plume transmittance is then given by

$$T_L = (A/B)^{1/2} \qquad (2.4)$$

All of this yields an absolute measurement of plume transmittance independent of laser pulse energy provided that k_s is homogeneous in front of and beyond the plume.

The above measurement is easy in principle, but in practice an accurate $1/t^2$ extrapolation of data to a common range is a time consuming nuisance. Also, a phenomenon called photomultiplier tube afterpulsing has previously limited the accuracy with which the signal on the far side of the plume can be read[1].

2.3 Range Correction

Since the lidar signal return, for a homogeneous scattering atmosphere, behaves inherently as $1/r^2$, it is necessary to transfer the data from a polaroid

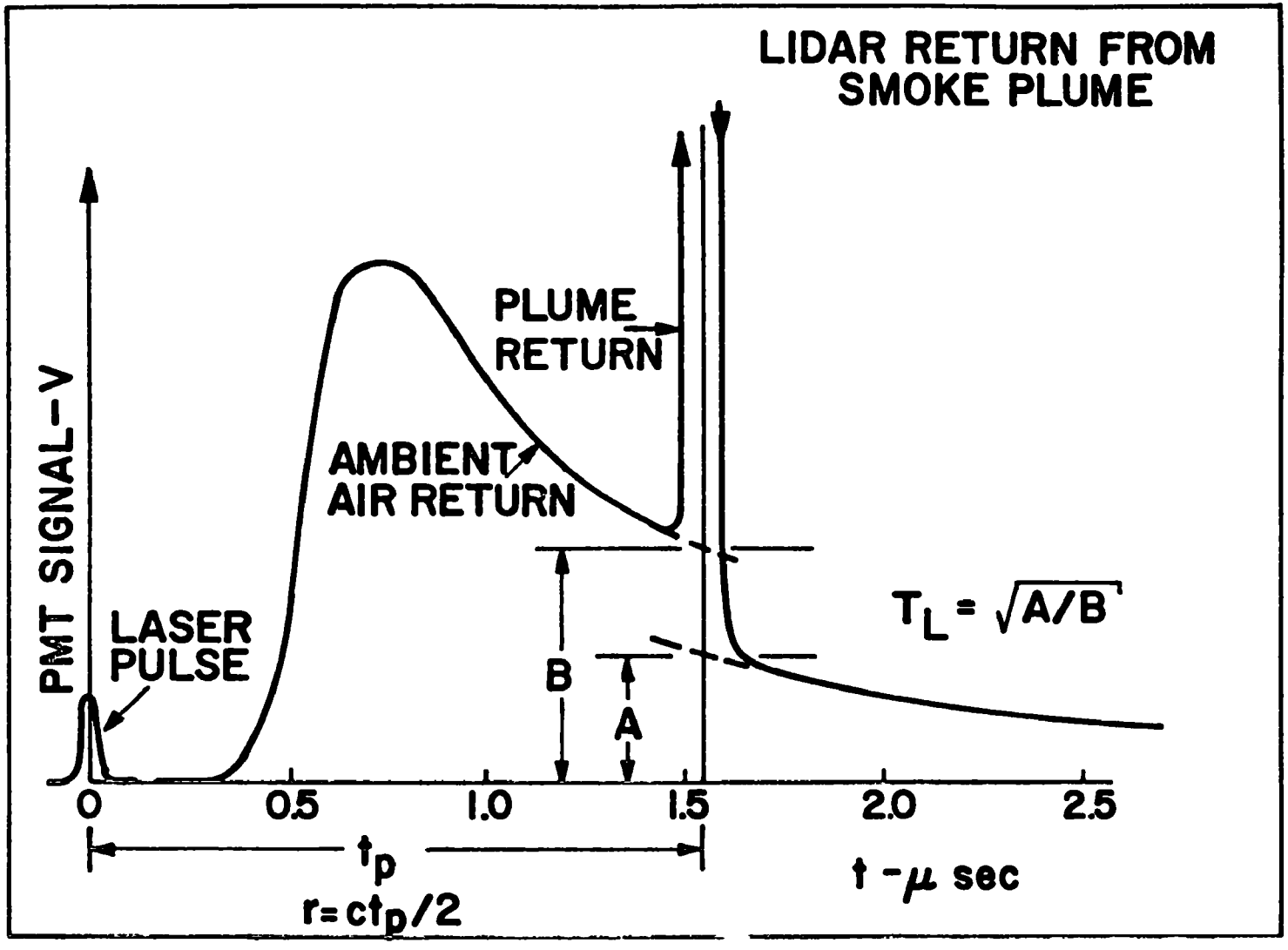

Figure 2.1 A sample lidar return through a smoke plume showing the single beam, single shot technique for obtaining the one way lidar determined transmittance, T_L.

oscillogram to a double logarithmic plot to make the necessary linear extrapolations prior to computing the far side to near side signal ratio, A/B. This is a time consuming process done with dividers and can take 20 to 30 minutes for one oscillogram before the results are known. If the signal were not $1/r^2$ in nature but constant with range, the data reduction could be done directly on the oscillogram simply by taking the ratio of the average signal level before and after the plume.

One method of range-correcting the $1/r^2$ lidar return to a constant signal output, is to run the output from the lidar receiver light detector through a t^2 amplifier and then on to the oscilloscope. The insertion of such an external amplifier into the system may reduce the detection frequency of response and it will have a maximum dynamic range of gain of about 100:1. However, such a separate t^2 amplifier has the advantages of being relatively easy to make, of not disturbing an existing detection system or interfering with the method of gating, and of being easily adjusted for use with different lidar range intervals. This is the type of range-correction system developed here (see Section 4).

2.4 Photomultiplier Tube Afterpulsing

In order to make lidar-determined smoke plume transmittance measurements, it is necessary to faithfully record the atmospheric backscattering both just in front of and just behind the plume. There is, of course, no trouble in obtaining the near side signal right up to the point in time where the laser pulse intersects the plume. However, the intense light scattering from the plume itself (during the time that the laser pulse is in the plume) complicates the problem of faithfully recording the clear air light scattering immediately on the far side of the plume. This backscattering from the plume can be as high as 40 db above the ambient clear air scattering for the case of a dense white plume (or for test purposes, a white wall).

As already indicated, an effect called photomultiplier tube (PMT) afterpulsing increases the apparent amplitude of the far side (of plume) clear air return, yielding plume transmittance values that are too high.[1] The explanation for this effect appears to be as follows: The PMT cathode photoelectrons (created by backscattered light from the intense plume return) leave the cathode and are accelerated towards the first dynode. At some point along their path these electrons acquire sufficient energy to ionize the residual gas in the tube or to eject ions from the tube structure upon impact. These relatively slow ions then are accelerated back to the photocathode where they cause secondary electron emission about 0.2 to 1μ sec. after the primary pulse. The secondary electrons then are amplified down the dynode chain and wind-up as an afterpulse signal at the anode. Those electrons resulting from light ion impact at the photocathode cause the earliest afterpulsing while heavier and slower ions cause the later afterpulsing. The amount of afterpulsing then depends on the intensity of the reflected signal from the plume or target.

As discussed in reference 1, attempts to stop the initial flow of plume-return photoelectrons by applying repelling electric fields to the PMT focus electrode, to an external grid, and to dynodes had not been successful. Some preliminary considerations had indicated that the best solution involves the use of a PMT that has been designed for off- and on-gating via an internal flat mesh grid located adjacent to and parallel to a flat photocathode. The PMT selected for this purpose is a specially designed grid-controlled tube (ITT type F4084) as described in Section 3.

2.5 Existing Lidar System Design

A detailed description of the lidar system design before this modification program, is given in reference 1. Figure 2.2 shows the lidar block diagram, while Table 2.1 lists many of the lidar optical characteristics.

To summarize here, the lidar transmitter consists of a Q-switched water-cooled ruby laser (with photodiode output monitor) beamed through a divergence-reducing 5 inch diameter Gallilean type collimating telescope. The lidar receiver consists of a 6 inch diameter telescope with 4 mrad. field of view and 12A FWHH interference filter (IF) located in front of the photomultiplier tube (PMT) detector. The original PMT detector was an Amperex 56TVP wired for an off-gating capability[1] to block the strong plume return signal. However, PMT afterpulsing[1] was still present to a degree sufficient to partially interfere with the far-side clear air return (see Figure 2.1), thus limiting the accuracy of the plume transmittance measurement. Data recording was accomplished with Polaroid oscillograms of the direct PMT signals.

This entire system is located in a motor van with flip open top and elevating lidar optics mount[1]. Portable motor generators provide electrical power when not otherwise available.

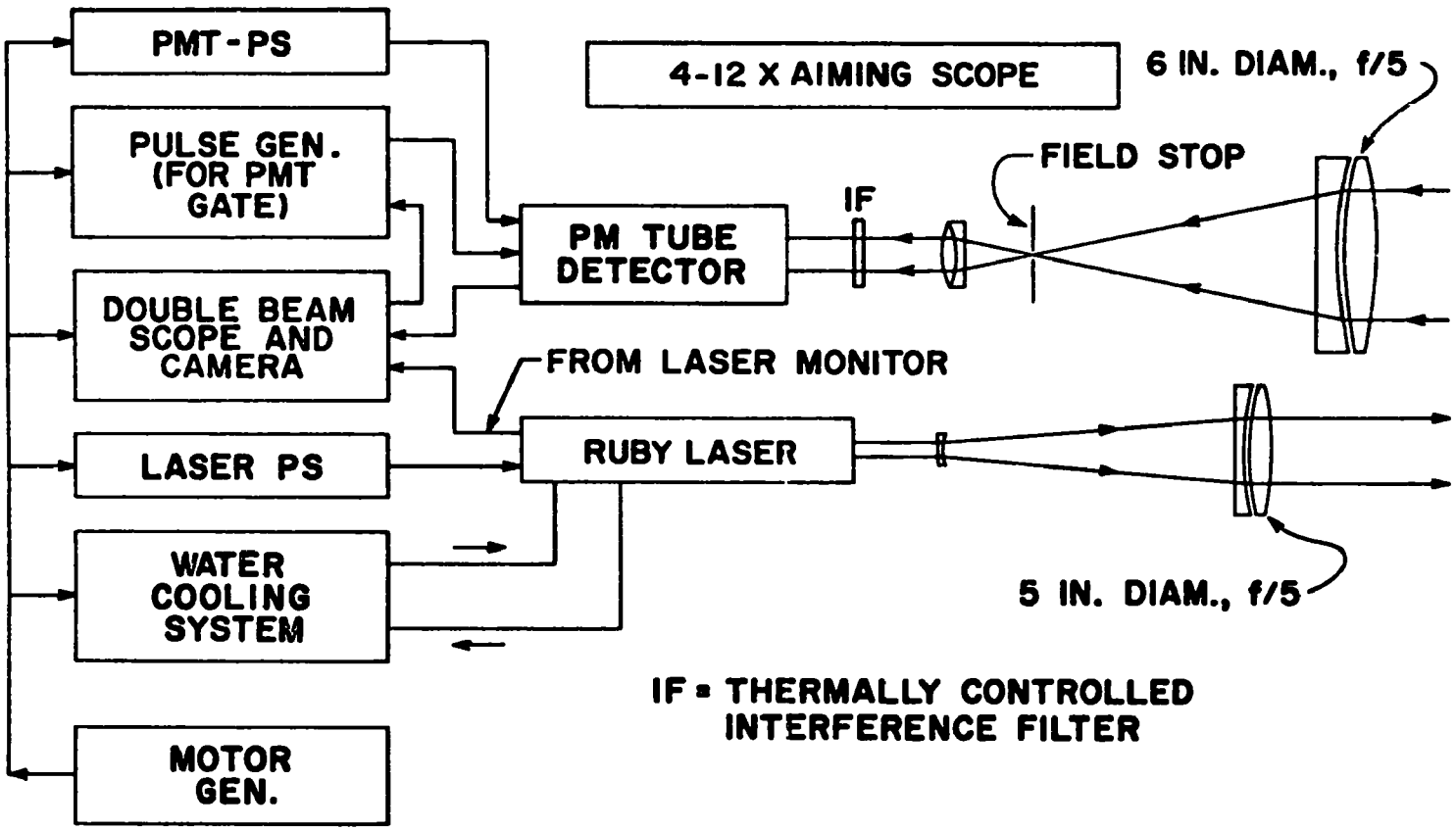

Figure 2.2 Block diagram of mobile lidar system

TABLE 2.1 Lidar Optical Characteristics

Laser

Manufacturer and Model:	Hadron/TRG Model 200B/104A
Type:	Rotating prism Q-switched ruby
Output Wavelength:	6943A
Maximum Output Energy:	1.0 joule Q-switched
Pulse Width (FWHH):	< 30 nanoseconds
Ruby Rod:	1.0 cm x 7.6 cm
Beam Divergence:	< 5 mrad. (full angle - 1/2 power)
Repetition Rate:	0 - 3 ppm
Cooling:	Deionized water

Laser Collimation

Collimated Beam Diameter:	10 cm
Collimated Beam Divergence:	~ 0.5 mrad. (full angle - 1/2 power)

Receiving Optics

Type:	Refracting
Objective Lens:	6 inch diameter, f/5
Collimating (eye) Lens:	2.14 inch focal length
Field of View:	4.0 mrad. full angle

Interference Filter

Manufacturer:	Infrared Industries
Type:	3 Cavity Interference
Diameter:	2 inches
Transmission Peak Wavelength:	6946.0A (25^{o}C)
Transmission Center Wavelength:	6943.4A (25^{o}C)
Thermal Shift:	+ 0.2 A/^{o}C
Bandwidth (FWHH)	12.0 A
Peak Transmittance:	0.66
Residual Transmittance:	< 0.01%
Filter Rejection:	Far uv to ≥ 1.0 micron
Filter Tilt in Lidar:	0^{o} (perpendicular to radiation)

3. USE OF GRID-CONTROLLED PM TUBE

3.1 Description of Photomultiplier Tube

An ITT type F4084 grid-controlled photomultiplier tube (PMT) was obtained for this lidar modification. Some of the manufacturer-supplied characteristics and test results for this particular PMT are listed in Table 3.1. It should be noted that all of the ITT tests were made using their standard (nearly linear) voltage divider, which is different from the more tapered divider designed for its use in this lidar system (see Section 3.2).

The principle feature of interest to us for this type PMT is that it has a mostly transparent internal flat mesh grid located parallel to and close to the flat multi-alkali photocathode. According to the tube manufacturer, this internal mesh grid not only permits off- or on-gating the PMT response to the incident light, but it is also likely to eliminate afterpulsing which results from any incident light during the off-period.

The flat photocathode and parallel flat mesh grid design reduces the tendency for charges to redistribute on the photocathode during the gating pulse. Furthermore, the tube manufacturer claims that the photocathode is of special low impedance design, thus reducing any charge distribution and current density problems. Consequently, no tendency was observed for the on-recovery time to increase as the off-gating period was increased to and beyond values of interest.

3.2 Divider/Gating Circuit Used

The special "tapered" PMT voltage divider designed for use with the lidar system, is shown in Figure 3.1. This divider system is significantly more tapered than the divider used by ITT because it was here desired to optimize linearity of PMT response to large pulsed outputs, even at the possible sacrifice of some PMT gain. To achieve a large pulsed output linearity requires both (1) increasingly large inter-dynode voltage differentials as the anode end of the tube is approached so as to reduce the current-limiting effect of space charge, and also, (2) increasingly large valued low inductance capacitors as the anode end of the tube is approached so as to maintain constant dynode voltages during the output pulse. It is at the anode end of the PMT where the amplified electron avalanche is largest and has the strongest disturbing effects which tend to upset linearity of response.

It should be noted that although the PMT is rated by the manufacturer to 6000 volts total, the maximum total voltage applied to this divider/gating circuit (Figure 3.1) must be limited to <3000 volts, and preferably should not exceed 2500 volts. The 3000 volt limit is dictated by the maximum voltage and dc wattage ratings of many circuit components, while a 2500 volt limit provides a safety margin for the 3000 volt gating pulse capacitors and also reduces heat produced in the divider circuit. Off-gate pulses of -5 volts are sufficient as discussed later.

Table 3.1 Manufacturer - Supplied Characteristics for ITT Type F4084 Grid-Controlled Photomultiplier Tube*

Tube manufacturer and type	IT&T F4084
Number of dynodes*	8
Multiplier type	linear focused
Photocathode characteristics:*	
Sensitivity type	MA-2 (modified S-20)
Quantum efficiency	4.8% at 6940A
Quantum efficiency	21% at 4080A
Tube response time	< 5 ns **
Grid gated on/off ratio*	43 db
Grid Δ V for on → off*	-2.5 volts
Maximum overall voltage	6000 volts **
Tube gain and dark current:*	

Overall voltage on tube	Tube Gain	Dark current (amps)
1000	2×10^3	1.2×10^{-10}
1500	2×10^4	4×10^{-9}
2000	1.2×10^5	6×10^{-8}
2500	5×10^5	7×10^{-7}
3000	1.7×10^6	5×10^{-6}
4000	9×10^6	----

Notes:

* These measurements were made by ITT on the supplied tube (S/N 077201) while using their standard (nearly linear) voltage divider.

** Based on the manufacturer's general specification sheet.

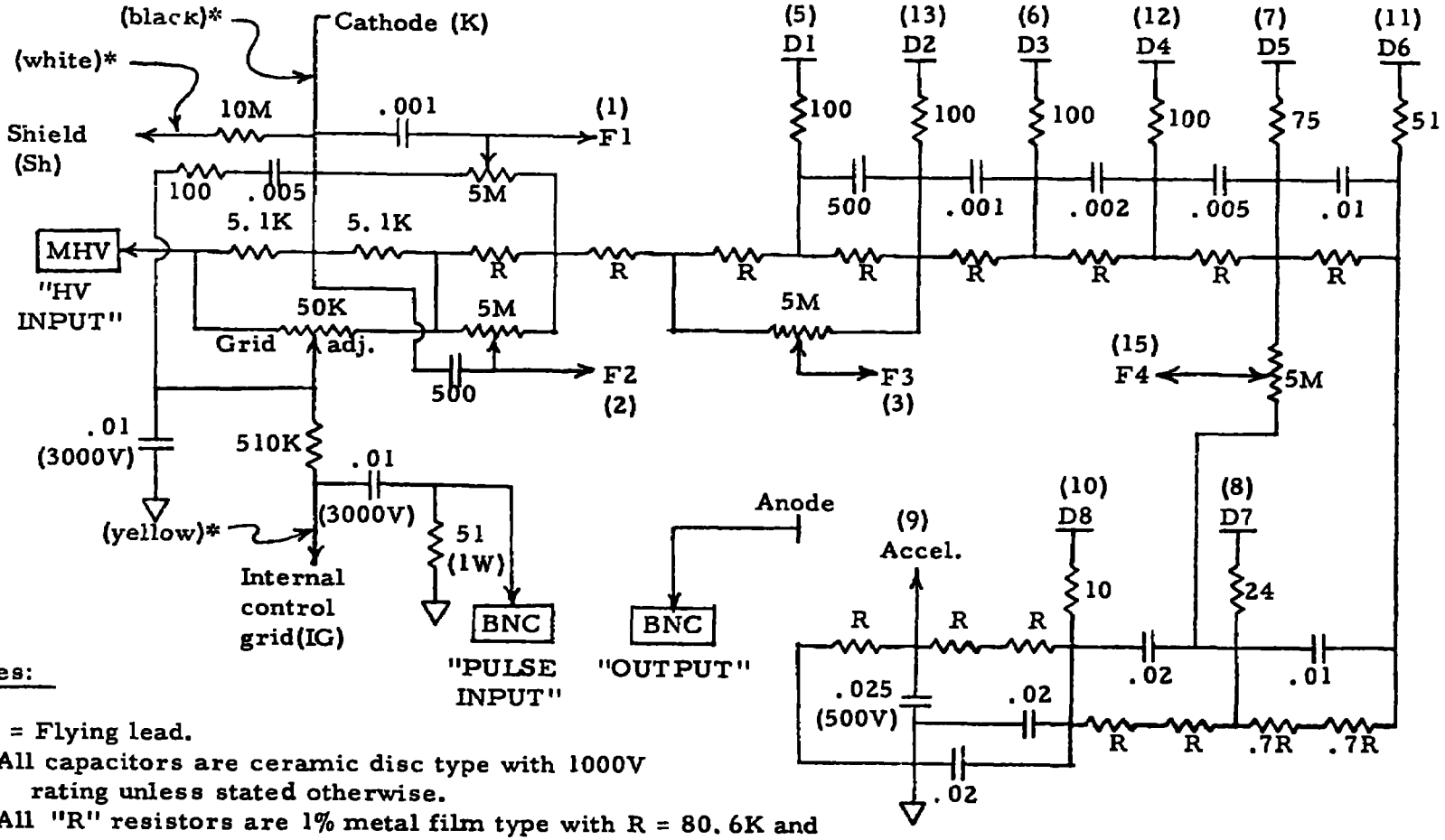

Notes:

1) * = Flying lead.
2) All capacitors are ceramic disc type with 1000V rating unless stated otherwise.
3) All "R" resistors are 1% metal film type with R = 80.6K and 0.7R = 54.9K.

Figure 3.1 Tapered voltage divider/gating circuit for the ITT type F4084 photomultiplier tube. Simple numbers in parentheses are tube pin numbers. The total divider resistance is 1.16 megohms.

3.3 Detection System Description and Performance

This F4084 photomultiplier tube (PMT) and housing are mounted in place of the originally used Amperex PMT and housing (see Fig. 2.2), while still using the original PMT power supply (PS) and gating pulse generator. A ground glass diffuser has been located between the PMT and interference filter IF (Fig. 2.2) so as to spread illumination of the PMT cathode over most of its area, thus optimizing its total current emission capability and reducing any effects due to variation of cathode sensitivity with spacial location.

Various new detection system performance characteristics and adjustments are presented in the following sub-sections.

3.3.1 Gain and Dark Current

Figure 3.2 shows plots of PMT gain and dark current vs. applied total voltage through the ranges of interest while using the divider circuit of Figure 3.1. These curves are based on room temperature measurements made at 100 volt intervals, with the dark current measurements being in amperes and the sensitivity measurements being relative while using a stabilized dc light source. To avoid dynode voltage dc distortions during these measurements due to high tube output, the light level was always such that the PMT anode current never exceeded .002 of the divider circuit current. The entire sensitivity curve was then normalized to a theoretical gain calculation of 2.29×10^4 at 1500 volts.

The above PMT gain (current amplification) was calculated for this particular tube as follows: First, a curve of gain/dynode (δ) vs. volts/dynode (Δ V) was derived from the manufacturer - supplied gain vs. voltage information (see Table 3.1) plus the voltage distribution of the divider circuit they used for those measurements. Then this δ vs. ΔV curve plus the voltage distribution of the divider circuit used here (Figure 3.1) was used to calculate the current amplification ("gain") at 1500 volts overall on the PMT. Thus, although the gain curve's shape and slope are accurately measured, its calculated normalization is less certain.

3.3.2 System Gating Characteristics

PMT gating response time and an approximately 20 db lower limit to on/off ratio was measured by off-gating the PMT while it was exposed to a stabilized cw light source. In these cases, a Corning #2412 red filter was used and the light level was adjusted to yield PMT anode outputs less than 0.1 of the divider chain current. The latter precaution insured reasonably linear PMT response under cw operating conditions. For all of these off-gate response time adjustments and measurements, a Tektronix #551 oscilloscope with #1A1 pre-amplifiers was used, this combination having a manufacturer - stated risetime (T_r) of 13-17 ns depending on scope sensitivity setting. The pulse generator

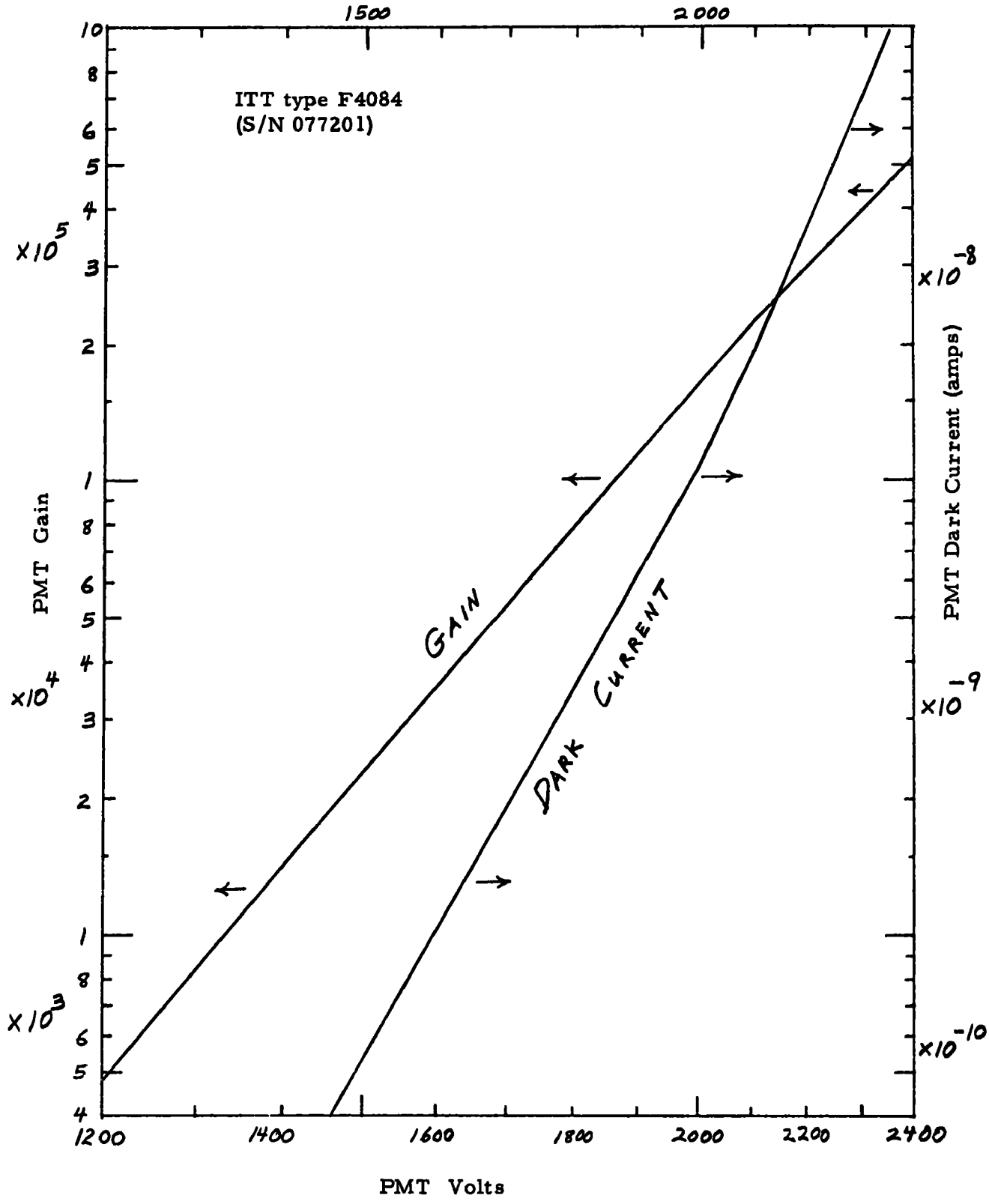

Figure 3.2 Photomultiplier tube (PMT) gain and dark current vs. overall voltage while using the "tapered" divider circuit of Figure 3.1 .

provided pulses of about 15 ns rise and fall times. Risetime (T_r) and falltime (T_f) are defined as the time required for the waveform to change from 10% to 90% of the final amplitude.

Satisfactory off-gating of this new detection system is obtained with gating pulses of -2 through -10 volts, with -5 volt pulses having been selected for all final gating investigations and adjustments. Since the optimum grid adjustment ("grid adj." of Fig. 3.1) is a moderate function of overall PMT applied voltage, the grid adjustment was optimized for $T_r \approx T_f$ at 1750 volts applied.

With all the above conditions and method of measurement, it was found that the detection system satisfactorily off-gates with an on/off ratio of at least 20 db, and both T_r and T_f are < 50 ns through the voltage range of at least 1550 - 1900 volts. It was also noted that the on-recovery time (T_r) is independent of off-gated period for gating periods to at least 1 microsecond in length.

Figure 3.3 shows oscillograms illustrating these off-gating measurements and results. PMT anode stray pick-up from the gating pulse produces the < 4 mV ringing in the PMT anode signal at the beginning and end of each gate pulse. This rapidly damped pick-up does not interfere with lidar useage of the detector due to their transient nature and due to the fact that the lidar signal amplitudes of interest are 10 to 1000 times greater than these pick-up amplitudes.

A more sensitive measurement than possible above of detection system gating on/off amplitude ratio was made by comparing an ungated but optically attenuated light pulse signal with a similar unattenuated but gated light pulse signal. This was accomplished by making monitored lidar shots at the white wall of a building. As illustrated in Figure 3.4, lidar returns were obtained from the white wall while not gating but with a 4.32 O.D. neutral density filter located in front of the detection system (Fig. 3.4a), and also lidar returns were obtained from that same white wall with no neutral filter but while off-gating (Fig. 3.4b). The neutral density filter is of the absorbing glass type, and had been calibrated at the laser wavelength. The examples of Figure 3.4 as well as other more sensitive oscillograms never clearly showed the wall return while off-gating, with the resultant conclusion being that the gating on/off ratio is at least 60 db.

Comparing these gating characteristics with those of the originally employed ("old") detection system (Amperex 56TVP tube with dynode off-gating), we see that the new detection system has $T_r \approx T_f = 40 - 50$ ns vs. ~ 35 ns for the "old" system[1], while the new detection system has an on/off amplitude ratio of ≥ 60 db vs. ~ 45 db for the "old" system[1].

3.3.3 Photomultiplier Tube Afterpulsing

PMT afterpulse investigations were made via white wall lidar returns similar to the on/off ratio lidar method just discussed above. The primary

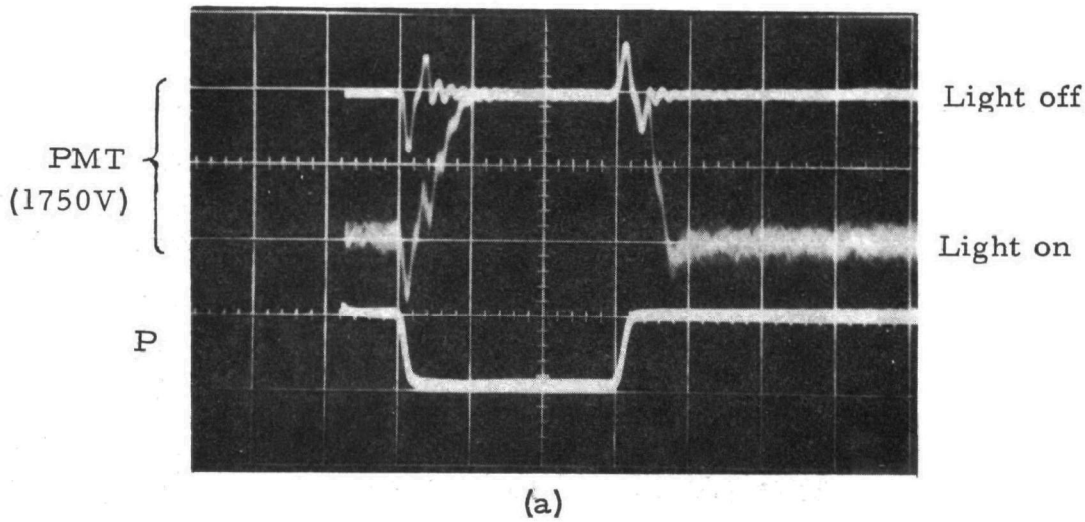

(a)

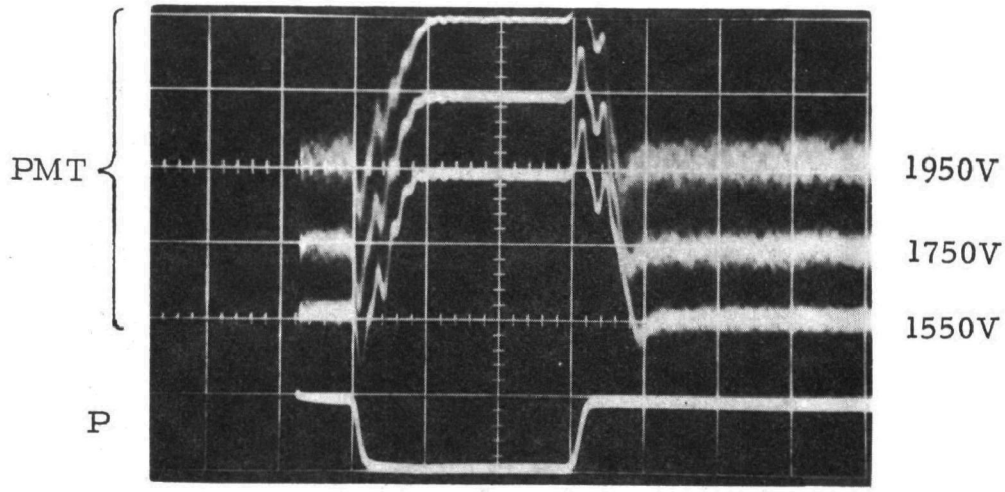

(b)

Figure 3.3 Double beam oscillograms showing response by the F4084 photomultiplier tube (PMT) to off-gating via divider/gating circuit of Fig. 3.1 in the presence of a cw light source. P shows the 300 ns long -5 V gating pulses at 5 V/cm, while the upper traces show the PMT response at 5 mV/cm through a 93 ohm cable and load under the conditions indicated, all with the control grid adjustment optimized for 1750 V operation. Scope sweep speed is 100 ns/cm.

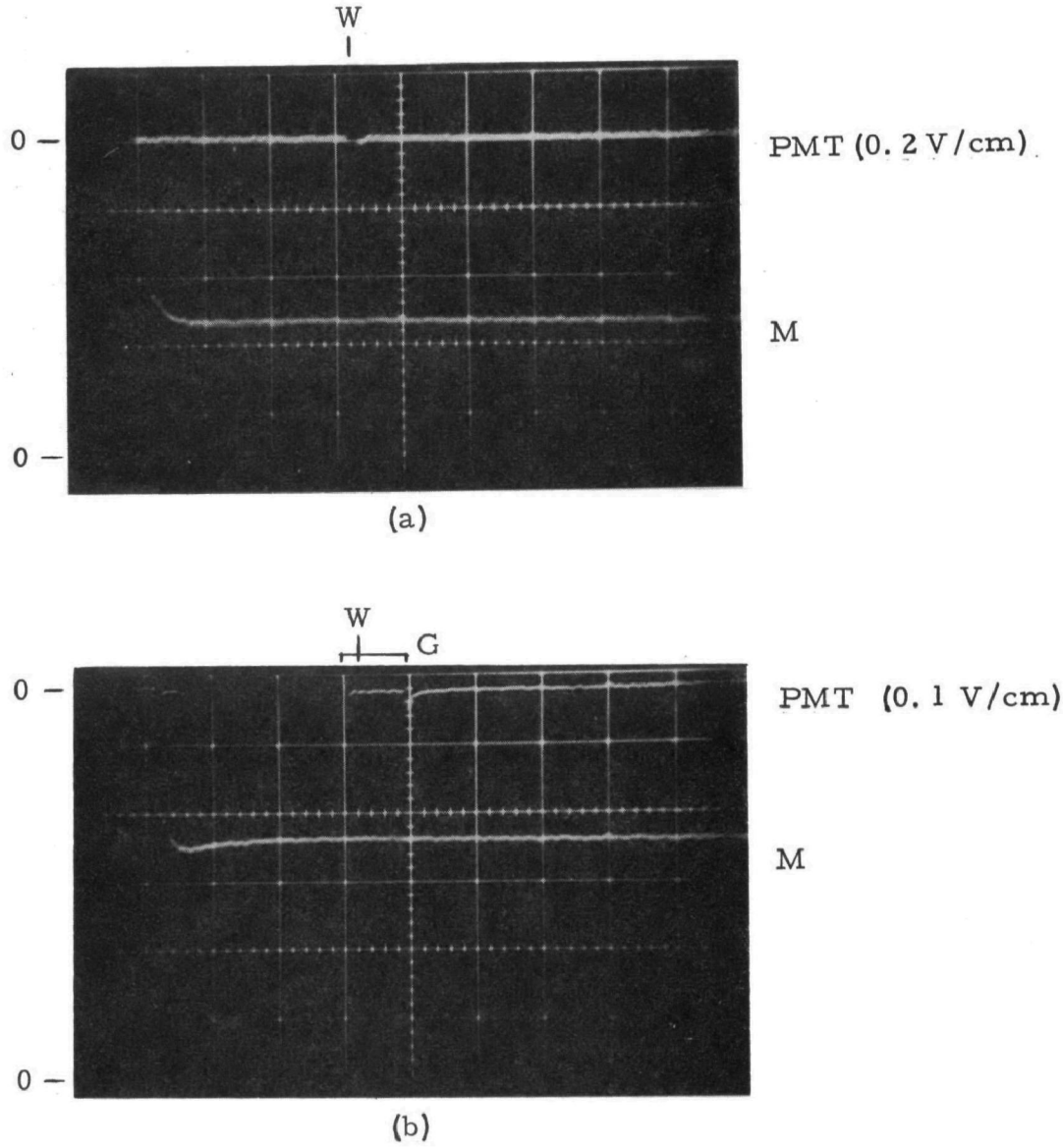

Figure 3. 4 Lidar returns from a white wall using the new detection system (F4084 PMT with circuit of Fig. 3. 1). In each double beam oscillogram, the sweep speed is 500 ns/cm, M is the positive-going laser energy monitor trace, PMT is the negative-going photomultiplier tube lidar return (PMT at 1700 V), and W is the position of the wall return. Figure 3. 4a has no gating but does have a 4. 32 O. D. neutral filter in front of the PMT yielding a wall peak return of -0. 8 cm, while Figure 3. 4b has no neutral filter but is off-gated through the 500 ns wide interval G with a -5V pulse. Except for such off-gating ratio measurements as these, much narrower off-gate periods were normally as illustrated elsewhere.

difference from the above measurements is that for the afterpulse measurements the non-neutral filter lidar shots were made with shorter off-gated periods and also with no off-gating.

These investigations showed this new PMT (F4084) to have generally weaker afterpulsing than the old PMT[1] (56TVP), and that afterpulsing which the new PMT does have ends much sooner after the primary (wall return) pulse. As illustrated in Figure 3.5a, the ungated F4084 after pulsing consists of a primary afterpulse peaking at Δt = about 200 ns after the primary pulse, and a weaker secondary afterpulse peaking at Δt just under 400 ns after the primary pulse. The secondary afterpulse then rapidly decreases at larger Δt. This ungated F4084 afterpulsing (see Fig. 3.5a) can be compared with the old PMT ungated afterpulsing as shown in Figure B1a of reference 1.

As seen by comparing Figures 3.5a and 3.5b, when the new detection system (F4084 PMT plus divider/gating circuit of Fig. 3.1) is off-gated, the white wall lidar return shows even less afterpulsing (A and A′) than when not off-gated. The residual off-gated afterpulsing can be seen at higher oscilloscope sensitivity in Figure 3.5c where the traces have gating conditions which are somewhat wider and later-ending than in the case of Figure 3.5b. These new detection system gated afterpulsing characteristics (Figures 3.5b and c) can be compared with the old (56TVP) detection system gated afterpulsing which is shown as Figure 3.1,reference 1 (Figure B1a of ref. 1 is also good for comparison because off-gating the old detection system does not influence its afterpulsing).

Finally, Figure 3.5d shows an off-gated clear air lidar return while using the new detection system.

Using the lidar method of Section 3.2.2, measurements of residual afterpuling by the off-gated new detection system shows the following results in terms of primary pulse (wall return)/afterpulsing amplitude ratio in db down vs. time delay (Δt) after the primary pulse:

Δt (ns)	~ 200	300	~ 360	500	> 700
ratio (db)	52	56	54	61	> 65

The ~200 ns peak is the primary (A) off-gated afterpulse, and the ~360 ns peak is the secondary (A′) off-gated afterpulse. Since the afterpulses themselves are also directly blocked during any off-gated interval, it may be that A actually peaks at Δt < 200 ns with a ratio of less than 52 db down.

3.3.4 System Linearity

PMT linearity of anode output can be limited by 4 effects: (1) Pulsed or dc output can be limited by photocathode charge depletion due to high incident light levels. (2) The dc or average anode current level can be limited by the

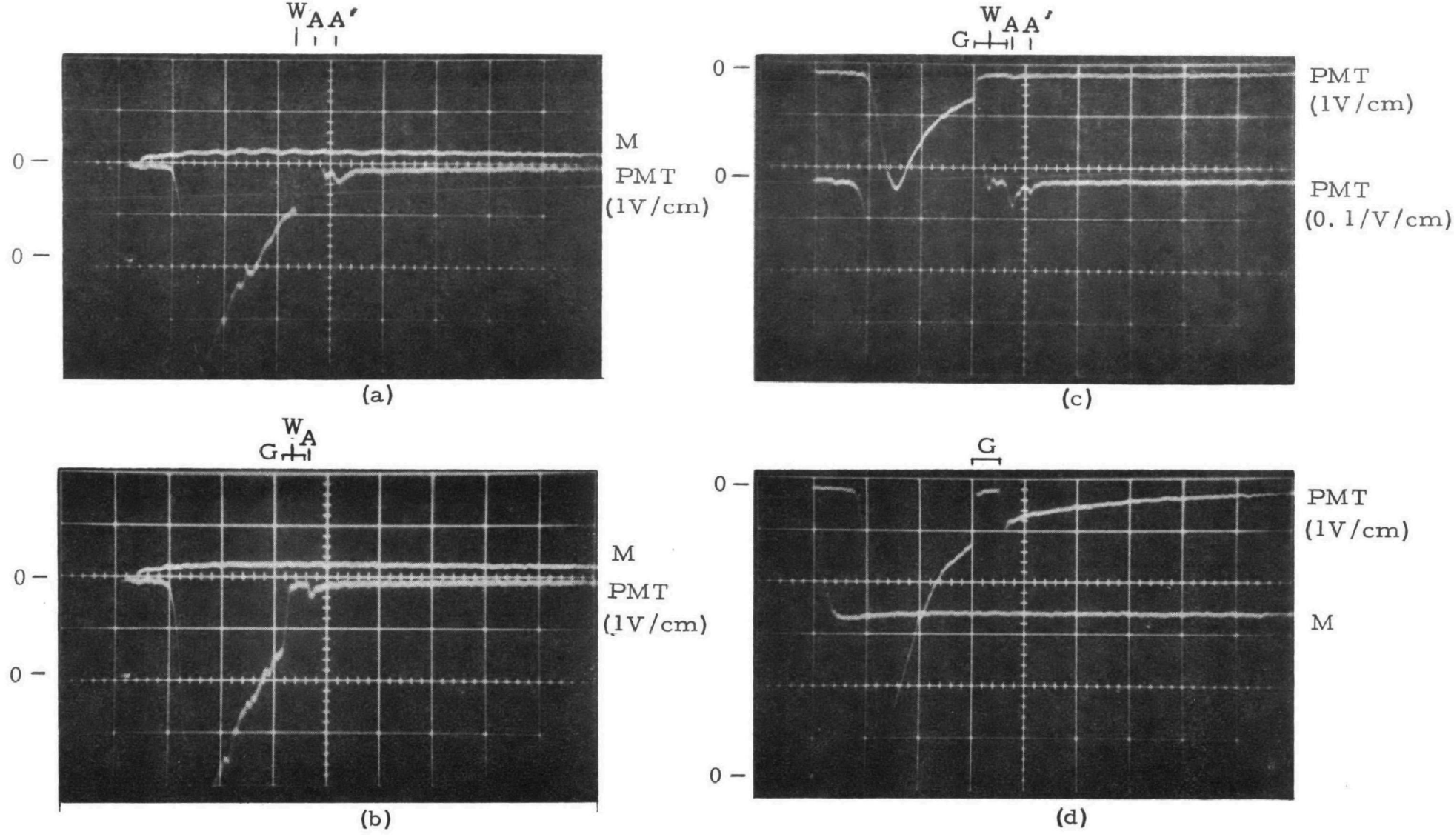

Figure 3.5 Oscillograms showing lidar returns from a white wall (3.5a to 3.5c) and clear air (3.5d) while using the new detection system (F4084 PMT with ckt. of Fig. 3.1). In each oscillogram, the sweep speed is 500 ns/cm, M is the positive-going laser energy monitor (ckt. modified between a & b and d), PMT is the negative-going photomultiplier tube lidar return, and W is position of the wall return. The primary and secondary afterpulse peaks are indicated by A and A′, respectively. Fig. 3.5a has no off-gating, while oscillograms b, c, and d have -5 V off-gating pulse widths through the intervals G of 200, 300 and 250 ns, respectively. Oscillograms a, b and c have 1700 V on the PMT, while d has 1800 V.

divider circuit current from which the output (anode) current must be obtained. (3) Low duty cycle or single pulsed current output can be limited by the charge stored in the dynode capacitors. (4) Pulsed current outputs can be limited by space charge effects, usually near the anode end of the dynode chain where inter-dynode currents are largest. The first through third limits above are due to induced distortions in the overall voltage distributions within the PMT.

The above linearity limits can be avoided or extended as follows: (1) Photocathode charge depletion can be avoided by limiting the PMT illumination density to low light levels and/or through the use of a low impedance photocathode design within the PMT. (2) The dc or average anode current limitation can be avoided by limiting the average anode output to < 0.05 of the divider circuit current. (3) The capacitor charge limit for pulsed use can be avoided by using large enough low inductance capacitors so they are < 0.05 discharged by the integrated current (i. e. charge) of the output pulse. (4) The space charge limit can be made less restrictive by employing larger PMT potentials and also by suitably arranging ("tapering") the voltage divider so that the inter-dynode potential differences (ΔV) increase down the dynode chain as the interdynode currents increase due to the current gain/dynode (δ). The space charge limit is approximately proportional to $(\Delta V)^{3/2}$.

For the intended normal lidar use of this new detection system, the combination of special low impedance photocathode in the F4084 PMT and the special tapered voltage divider (Fig. 3. 1) with relatively low overall resistance and large low-inductance capacitors results in only the space charge effects (#4 above) limiting the detection system linearity.

Measurements were made of space charge-limited linearity as follows: A pulsed light source with pulse widths of 1 microsecond (FWHH) and a repetition rate of 105-125 cps was produced by reflecting a stabilized HeNe laser beam (6328A) off a rapidly rotating mirror. This sweeping laser light beam was then intercepted by (1) various calibrated neutral density absorbing glass (not coated) filters, (2) a wide "slit" to spacially limit the period of light, (3) a ground glass diffuser to spread illumination uniformly over the PMT photocathode, and (4) a Corning red filter to reduce unwanted background illumination. The cw signal level plus pulsed light duty cycle were such as to limit even the maximum average anode output to < 0.01 of the divider current.

This space charge-limited linearity measurement was made, as detailed above, at both 1500 volts and 1800 volts PMT potential. The space charge-limited actual anode outputs for 2%, 5% and 20% deviations (decreases) from a linear response are listed below for these two PMT potentials and as interpolated for some nearby potentials: The voltage values assume a 93 ohm load.

PMT volts		1500	(1600)	(1700)	1800	(1900)
Percent dev. from linear.	Actual anode output					
≤ 2%	max. volts	1.8	2.1	2.4	2.7	3.0
	max. ma	19	22	26	29	32
5%	volts	2.1	2.4	2.7	3.0	3.3
	ma	23	26	29	32	36
20%	volts	3.5	3.8	4.1	4.4	4.7
	ma	37	41	44	47	51

4. TIME-SQUARED AMPLIFIER

As previously indicated, a time-squared amplifier has been developed to range-correct (linearize) the lidar return as received from the lidar photomultiplier tube detector.

4.1 Amplifier Design

The time squared amplifier (TSA) circuit is shown as Figure 4.1. The basic concept of the circuit is to use a linear ramp plus analog multiplier M1 to first provide a time-squared ramp (and thus range squared - see Section 2.1), and to then combine this t^2 output from M1 with the amplified photomultiplier tube signal (from operational amplifier A521) in a fast analog multiplier M2, yielding from M2 a signal constant with range for a homogeneous scattering atmosphere.

Still referring to Figure 4.1, the detailed operation is as follows: The linear ramp which feeds M1 is derived from the 0 to + 150 volt sawtooth output from the same oscilloscope (or any linear ramp generator) which is triggered by the lidar laser monitor and which can also receive the TSA output if desired. Because M1 and M2 each have a maximum input of 10 volts, the linear ramp is reduced in amplitude, and selected by the "Far Limit" potentiometer to reach 10 volts at any desired fraction of the total linear ramp. A protective diode located near T5 in Figure 4.1 limits the voltage reaching M1 to a maximum of 10 volts to avoid overdriving M1. Since these multipliers both have outputs which are XY/10, the linear ramp input to both X and Y of M1 yields a ramp-squared (t^2) output with a maximum of 10 volts. This t^2 output ramp from M1 (at T6) is then multiplied in M2 with the amplified and inverted lidar PMT output so as to yield the range-corrected output. The variable dc input level applied at T4 of Figure 4.1 allows fine adjustment of the ramp time-zero so as to optimize the "flatness" of the final range-corrected output.

The negative-going photomultiplier tube ("PMT") lidar output current passes through a 93 ohm load resistor (between T1 and T2 of Figure 4.1) to the 100 Mc (gain bandwidth product) inverting operational amplifier A521. Since such operational amplifiers maintain their input (T2) at a virtual ground potential, the 93 ohm resistor at T1 results in a proper impedance match for the RG62/U coaxial cable used from the PMT. The amplification factor of A521 is controlled by the feedback resistors selected by the "Gain" switch to be nominally 3X, 5X, or 10X. The 300 ohm and 4-25 pf RC pair in each feedback loop permits separate optimization of the A521 fast response at each gain setting. The amount of amplifier gain chosen is based on the PMT output voltage (at T1) at the nearest lidar range of interest. Because both the A521 maximum output and the M2 maximum input are each 10 volts, the 3X, 5X, or 10X "Gain" setting will determine whether the near range limit for t^2 operation is at a PMT output voltage (at T1) of about 3V, 2V, or 1V, respectively. The "Mode" switch merely permits bypassing the entire TSA while providing the proper 93 ohm load.

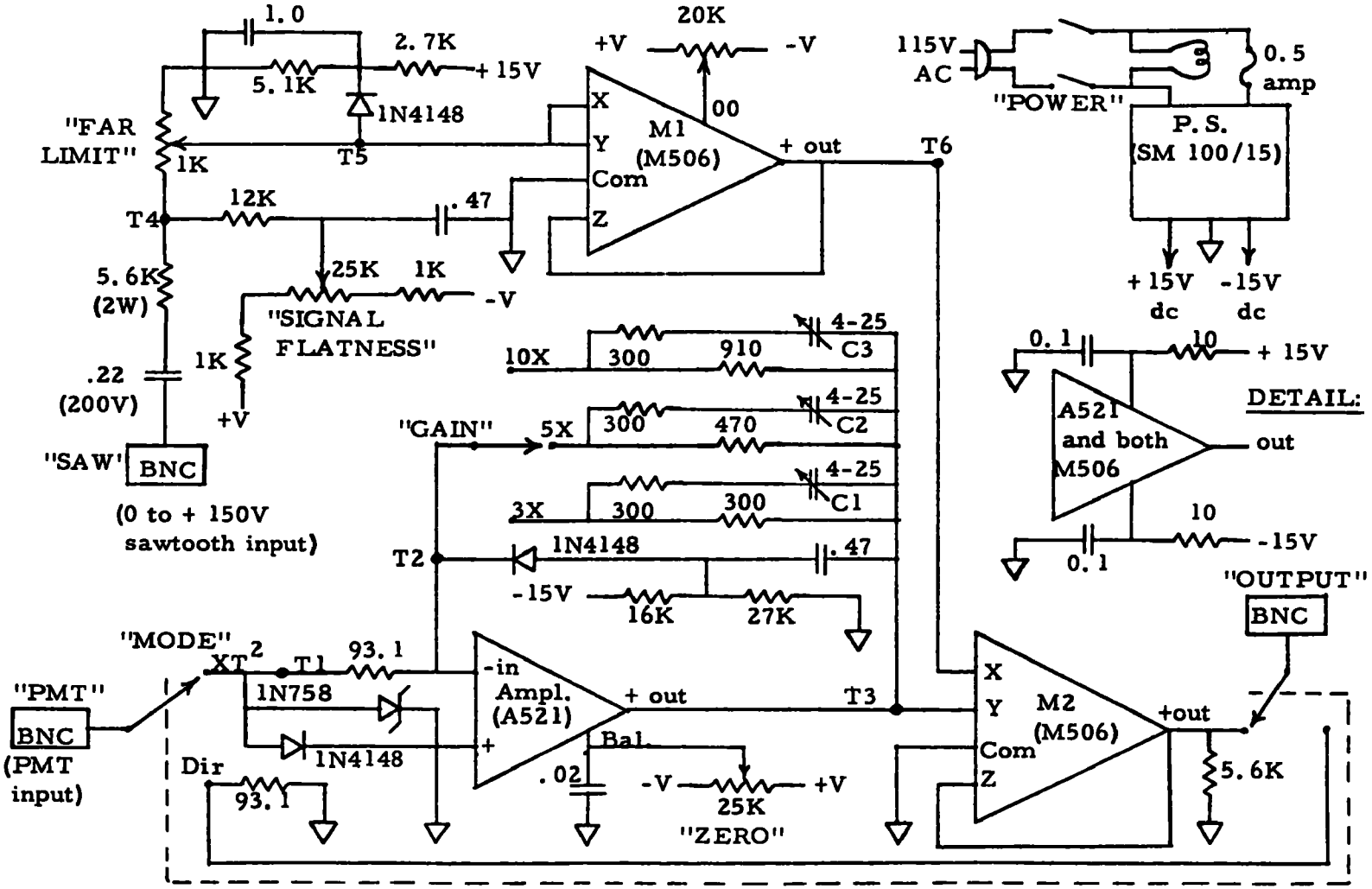

Figure 4.1 Time-squared amplifier circuit for range correction of lidar return.

To permit the PMT output voltage to exceed the above values of 3V, 2V, or 1V (depending on A521 gain) without overdriving or damaging amplifier A521, an automatic output limiting feature was added to the A521 circuitry. When the A521 output reaches 10 volts and therefore approaches saturation, the diode-containing section of its feedback circuit reduces the amplifier gain so as to maintain its output at 10 volts. By preventing saturation and even possible damage, this feature permits immediate recovery (in < 100 ns) from what would otherwise be too large a voltage at T1, as is always the case when the lidar near range of interest is beyond the lidar return maximum. The diodes from T1 to ground merely provide further protection against really large negative voltages (> 10 V) at T1 and against any positive voltages accidentally applied to T1.

4.2 Amplifier Performance

The time-squared amplifier (TSA) was first adjusted and tested in the laboratory, followed by field tests on the lidar system.

With TSA capacitors C1, C2, and C3 (Fig. 4.1) adjusted for the best overall performance of amplifier A521, the 10% to 90% risetimes and falltimes (T_r and T_f, respectively) were measured for both amplifier A521 and also for the TSA overall (i.e. for the A521 and M2 in series). For the latter measurements, a time squaring effect was avoided by applying 4.5 volts dc at T5 (Fig. 4.1), yielding about 2 volts dc at T6. Oscillograms for these measurements are shown as Figure 4.2, with the measured $T_r = T_f$ values being $\leq$ 15 ns, $\sim$ 16 ns, and $\sim$ 30 ns for amplifier A521 at 3X, 5X, and 10X gain, respectively; and $T_r = T_f = \sim$ 70 ns (about 5 Mc bandwidth) at all three gain settings for the TSA overall. The oscilloscope risetime of $\sim$ 13 ns and pulse generator risetime of "< 13 ns" limited the A521 measurements. The ringing seen at the leading and trailing edges of the applied square wave (at T1 of Fig. 4.1) are due to the fact that the 93 ohm input at T1 of Figure 4.1 did not match the 50 ohm output and cable from the pulse generator.

When the time squared amplifier (TSA) is incorporated into the lidar system (including the new F4084 PMT), its clear air performance is shown in Figure 4.3. Here and elsewhere, a BNC Tee connector at the TSA input plus a short length of extra cable to the oscilloscope permits simultaneous recording of both TSA output and TSA input (PMT output). Fig. 4.3a and b show the clear air return to be properly range corrected when the "Signal Flatness" (see Figure 4.1) is correctly adjusted, while Figures 4.3c and d show the distortions introduced by opposite extremes in mis-adjustment of "Signal Flatness". In each case, the near range correction is properly initiated (N in Fig. 4.3) at that point where the product of PMT output volts times TSA gain setting equals 10 volts. Any nearer range excess PMT output voltage is accepted by the TSA without impedance matching or recovery problems.

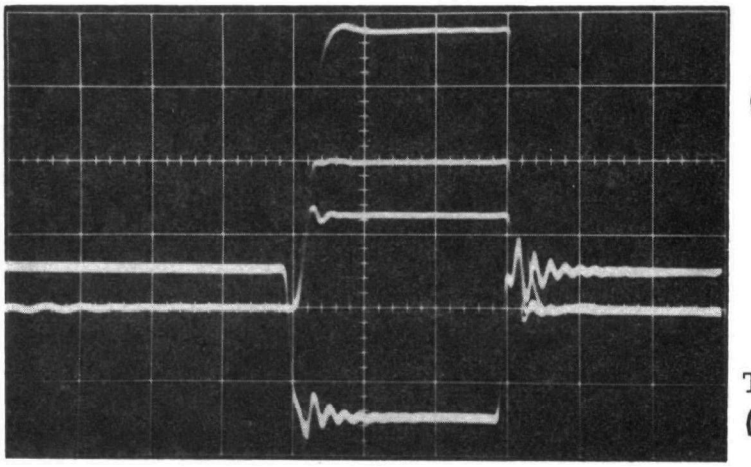

(a)

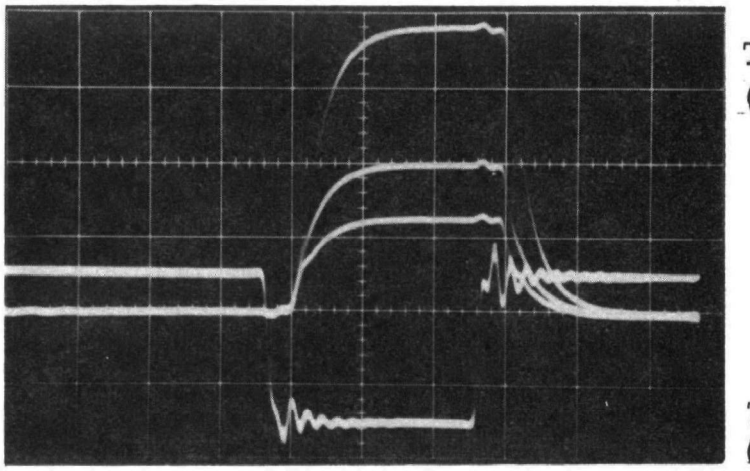

(b)

Figure 4.2 Double beam oscillograms showing time-squared amplifier (TSA) response. Sweep speeds are all 100 ns/cm. The lower (negative-going) trace of each oscillogram shows the applied test pulse at the PMT (T1 of Fig. 4.1). The upper (positive-going) traces of each oscillogram show the A521 amplifier response (probe at T3 of Fig. 4.1) and the overall response (at TSA "output"). In each case, the upper trace shows the superposed outputs at TSA gain settings of 3X, 5X, and 10X (see Fig. 4.1). As described in the text, the TSA "output" is here not multiplied by time squared.

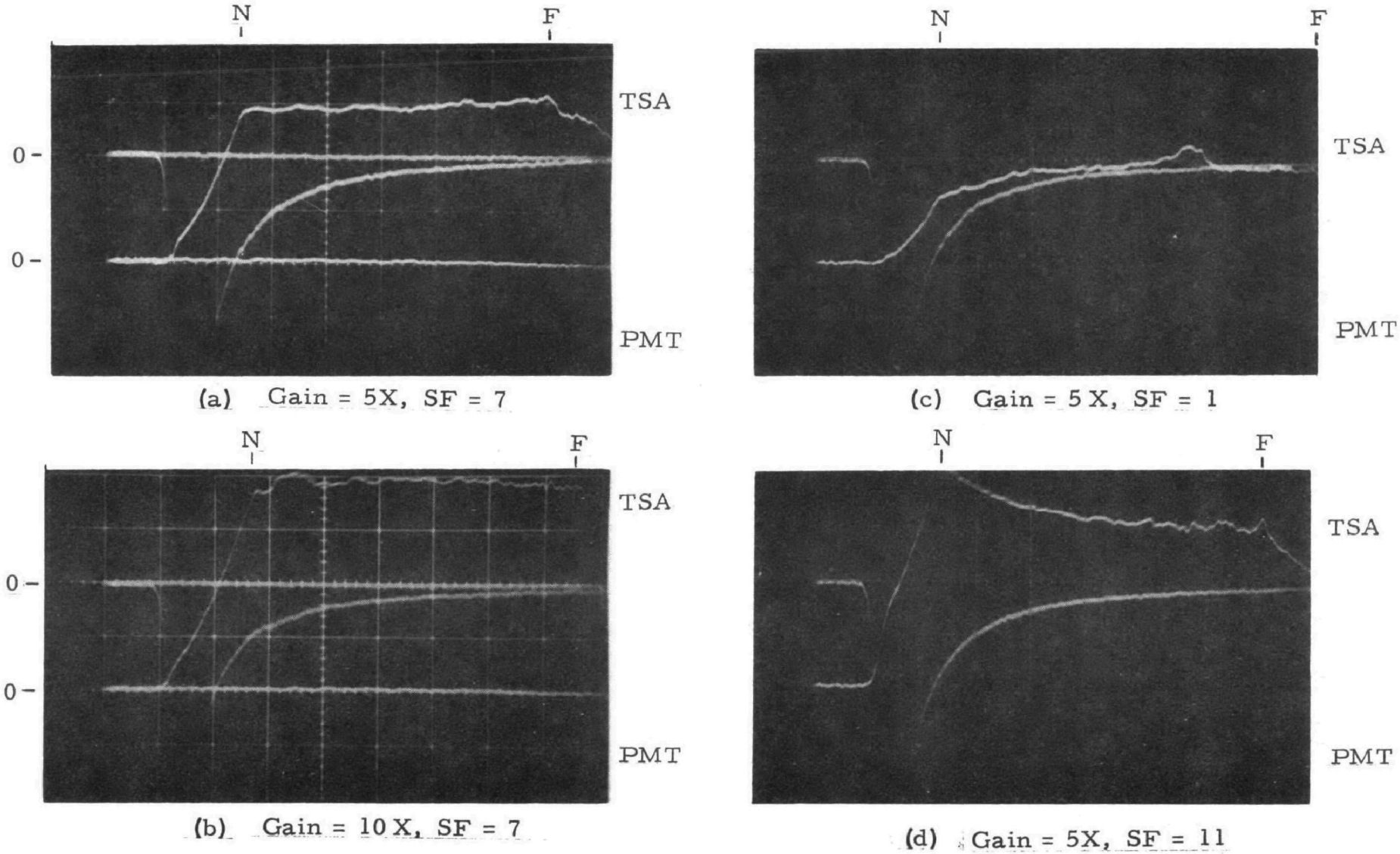

Figure 4.3 Double beam oscillograms showing time-squared amplifier (TSA) lidar returns from relatively homogeneous clear air. Each oscillogram is externally triggered by the laser monitor (not shown), and has a sweep speed of 500 ns/cm. In all cases, the negative-going lower trace (at 1 V/cm) is PMT input to the TSA, while the positive-going upper trace (at 0.2 V/cm) is TSA output. The TSA output range correction starts at N and ends at F. Under each oscillogram is listed TSA gain setting and "signal flatness" setting (SF). Figure 4.3a and b additionally show zero signal traces.

Figure 4.4 illustrates the general performance of the TSA under three extremes of lidar operation. Figure 4.4a shows the TSA response to off-gating the F4084 PMT (260 ns gate) during a lidar shot into clear air. Figure 4.4b shows the TSA response (plus PMT response) to a lidar shot at a white wall located about 800 feet from the lidar system while off-gating the F4084 PMT (250 ns gate). The zero signal trace shows very little effect due to PMT after-pulsing or electronics recovery. Finally, Figure 4.4c shows the TSA response to a lidar shot at the same white wall (same range) while not off-gating the F4084 PMT. In this severely fast overvoltage case, we see that the TSA over-voltage protective mechanisms are not able to prevent slow recovery and ringing. Here, TSA recovery requires about 800 ns, and even then comparison with the TSA zero shows some small tendency for signal wander at the right edge of the trace. The apparent ringing of the PMT return in Figure 4.4c is due to the above-discussed severe overvoltage effect on the TSA, resulting in the TSA temporarily not being able to maintain a proper 93 ohm load for the PMT and its cable. The PMT itself recovers much faster than shown in Figure 4.4c from an ungated white wall return (see Fig. 3.5a).

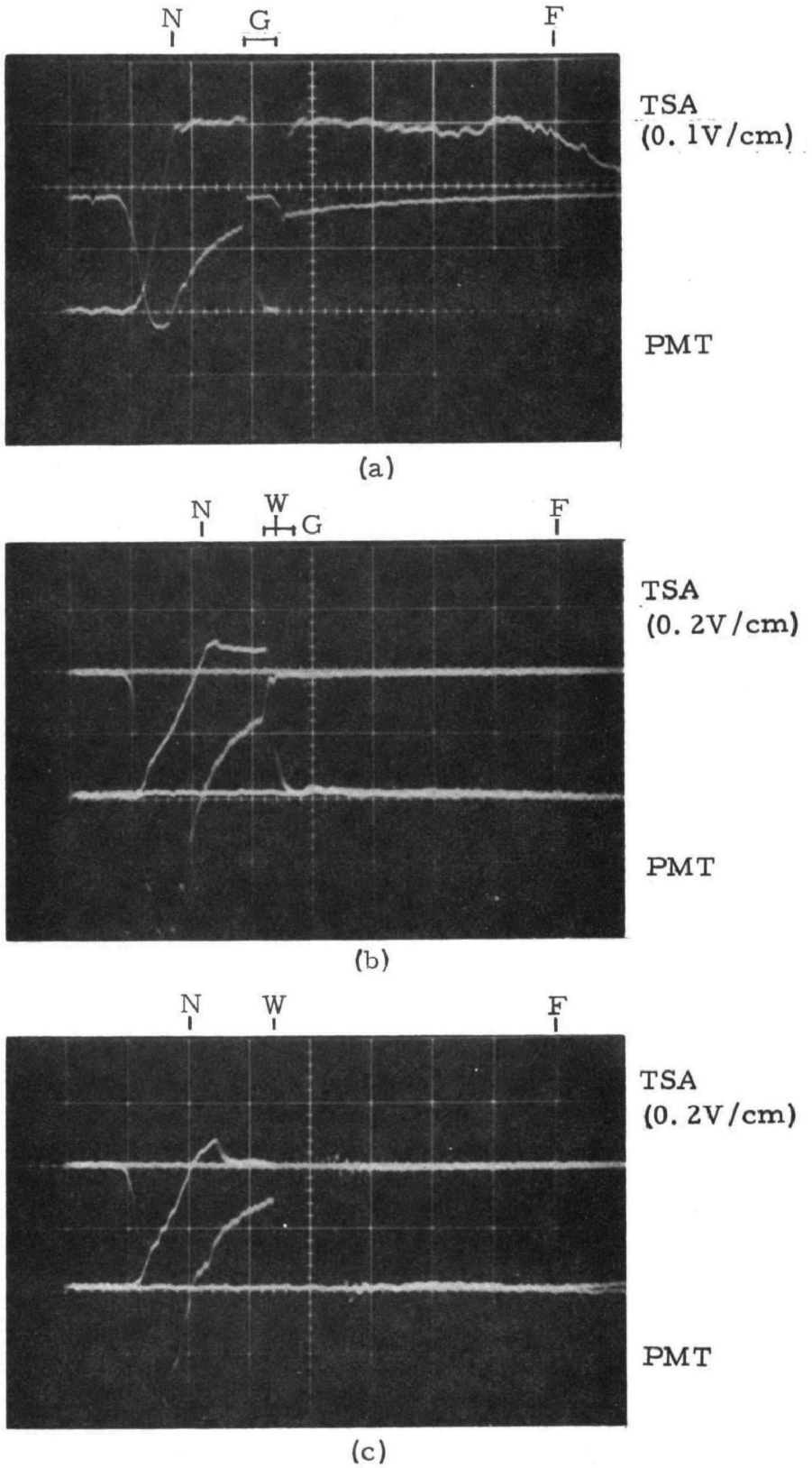

Figure 4.4 Double beam oscillograms showing time-squared amplifier (TSA) performance under three extremes of lidar operation. Each oscillogram is externally triggered by the laser monitor, and has a sweep speed of 500 ns/cm. In all cases, the negative-going lower trace (at 1V/cm) is PMT input to the TSA, while the positive-going upper trace is TSA output with TSA gain at 5X. Off-gating intervals (250-260 ns) are indicated by G, white wall position by W, and the near and far limits of range correction by N and F, respectively.

5. LIDAR MEASUREMENTS OF TEST TARGETS

After incorporation of the new (F4084) photomultiplier tube (PMT) and the time-squared amplifier (TSA), the modified mobile lidar system was evaluated using glass, Plexiglass, screen, and opaque test targets at a range of 216 meters. These lidar measurements and also laboratory re-measurements of the original test targets were made using methods and locations similar to those previously reported in reference 1.

5.1 The Test Targets and Their Laboratory-Measured Transmittances

As discussed in reference 1, the test target holder has a clear circular aperture of 42 inches diameter, with the test targets themselves being 42-45 inches square. As indicated above, these glass, Plexiglass, aluminum screen, and opaque targets are from those originally used[1] for both laboratory and lidar measurements in 1971. The 1/4 inch thick Plexiglass-G was manufactured by Rohm and Haas, and the 1/4 inch thick Parallel-0-Float glass was manufactured by Libby-Owens-Ford.

These new "laboratory" transmittance measurements were made[1] by illuminating the targets from one side with a collimated white light source while viewing the source from the other side of the target with the lidar receiving system. The targets were alternately placed in and out of the beam while the PMT (original lidar Amperex 56 TVP) output was read directly on a Keithly electrometer. This procedure was repeated with the same light source blocked off to permit subtraction of the small PMT dark current and target front lighting signals. Because the lidar receiver bandpass filter is centered at 6943 A, the laboratory transmittance measurements were made at the same wavelength as the lidar laser output.

In the course of these new transmittance measurements, it was noted that the originally used[1] "collimated" light source was actually very poorly collimated (about 115 mrad full angle). The use of such a poorly collimated source should have no significant effect on the absorbing target (glass & Plexiglass) results, but it should lead to screen target transmittance results which are too large. This is because non-collimated (angled) incident light rays which should not be accepted by the receiver (itself collimated to 4 mrad full angle), can reflect off the screen wires to produce rays which are at such an angle as to be accepted by the collimated receiver. These rays are in excess over those which are desired for a correct measurement, and thus yield transmittance values which are too large.

Due to the above reasoning, the new target transmittance measurements were made with both the originally used[1] poorly collimated light source ($\sim$ 115 mrad), and also with a different and much better collimated light source ($\leq$ 2 mrad full angle). The results of both old and new transmittance measurements

are shown in Table 5.1. Since the collimated light sources both had beam diameters of 2 inches, and the target clear diameter for lidar measurements is 42 inches, all measurements were made near the target centers where the lidar transmittance measurements were normally made. The highly collimated measurements were also made at many locations over the entire clear target area as a check on target uniformity.

As seen from Table 5.1, both the old and new 115 mrad collimator-determined screen transmittances are in relatively good agreement, while the good collimator-determined screen transmittances are significantly smaller. This is especially true for the "30%" screen which has a high ratio of wire area to clear area. As expected, we also see that the quality of source collimation has little if any effect on the measurement of non-screen targets. The slightly smaller transmittance recently measured for Plexiglass as compared with the original measurement, may be due to the effects of aging. Of the various target materials employed, it would seem that Plexiglass should be the most susceptible to aging.

5.2 Lidar Transmittance Measurements of Test Targets

As discussed above and in reference 1, the 42 inch diameter target holder was placed on the roof of a small building at the Valley Forge Space Center at a range of 216 meters, in the same manner as was used for the 211 meter tests of reference 1. The target holder was arranged so that any specular reflection was off axis, and the lidar system was aligned so that the transmitting and receiving axes crossed at the target range. This was not really necessary, but it facilitated aiming the system and was easy to do. A lidar shot through the center of the empty target holder showed no trace of a target holder return pulse such as would be obtained from even a fractional percent of the laser beam energy hitting the inside edge of the target holder.

In the above manner, each target was measured three times using the PMT gated and often also once with the PMT not gated. In each case, the oscilloscope was triggered externally by the laser monitor, with each oscillogram recording both t^2 amplifier (TSA) output and TSA input (via a BNC tee connection at the amplifier input plus a short cable to the scope). For all of these test target measurements, the TSA gain was set at 5X. Thus the oscillograms were similar to those extreme cases shown in Figure 4.4 as well as intermediate cases to be shown later.

Since the TSA output is range compensated, the lidar-determined target transmittance (T_L) is (see equation 2.4)

$$T_L = (A/B)^{1/2} = (V_f/V_n)^{1/2} \qquad (5.1)$$

where V_f and V_n are oscillogram voltages from the far side and the near side, respectively, of the target. Since the transmittance measurement depends on homogeneous atmospheric scattering, the results should be most reliable if the

Table 5.1 Summary of Laboratory-Measured Target Transmittances at 6943 A

Measurement	Old* (1971)	This contract		
Source collimation (mrad full angle)	~ 115	~ 115	≤ 2	
Portion of target	Center	Center	Center	Overall
Target:				
Plexiglass-G #1	.915	---	---	---
Plexiglass-G #2	.915	---	.903	.897-.908
Glass	.861	---	.858	(uniform)
Al insect screen #1	.640	.644	.604	.599-.611
Al insect screen #2	.645	---	---	------
50% Al screen	.515	.523	.486	.470-.500
30% Al screen	.288	.292	.192	.180-.195

* See reference 1

near side and far side measurements are made as close to the target as possible. This closeness is limited by (a) the PMT off-gate width used, (b) the detection electronics recovery time, and (c) also by the small afterpulsing which even this new PMT has.

Although this new PMT (ITT F4084) has weaker and shorter-lived afterpulsing than does the old PMT (Amperex 56TVP), the V_f measurement should still preferably be made after the afterpulsing has decayed. Oscillograms from white target lidar measurements show the major afterpulsing to be decayed within 0.3 μ sec after the target return, with nearly complete decay requiring 0.6 μ sec after the target return. This is further discussed in Section 3.3.3 and illustrated in Figure 3.5.

During the day of these test shots (12/1/72, weather clear, cool and windy), the atmospheric scattering uniformity often changed very rapidly from good to bad and back again. Use of the TSA makes the presence of these non-uniformities very obvious. For the lidar shots made during these target tests, the atmospheric uniformity was relatively good about 1/2 of the time, fair about 1/3 of the time, and poor (shots not useable) about 1/6 of the time. This problem of atmospheric uniformity provides an incentive for making the lidar measurements as close to the target (or smoke plume) as is consistent with the system performance discussed above.

With all the above considerations in mind, the lidar oscillograms of test targets were measured as follows:

1. For comparison, V_f was measured during four different time intervals (Δt) after the target,
   (a) from the average return during $\Delta t = 0.25 - 0.55\ \mu s$
   (b) from the average return during $\Delta t = 0.65 - 0.9\ \mu s$
   (c) from the average return during $\Delta t = 0.9 - 1.9\ \mu s$,
   (d) from extrapolation to target time of the return after $\Delta t = 0.65\ \mu s$.
2. In all cases V_n was measured from the average return during 0.1 - 0.4 μ s before the target.

For each measured range interval, the average lidar transmittances from all similar lidar shots are listed in Table 5.2 along with the average deviation of individual transmittance measurements from the listed averages. For comparison, Table 5.2 also lists the earlier (1971) average lidar transmittance values[1] and the recent highly collimated laboratory measurements of target center transmittance as listed in Table 5.1. Most of the results shown in Table 5.2 are plotted in Figure 5.1.

Table 5.2 Averaged Results of Recent Lidar Measurements of Target Transmittance.
(See Figure 5.1 for plot)

Target	Gated off?	1971 Lidar Transm.[1]	Recent Lab. Transm.	Recent Average Lidar Transmittance* (modified lidar)				
				No. Shots	Δt (μs)= .25-.55	Δt (μs)= .65-.9	Δt (μs)= .9-1.9	Δt (μs) = extrap > .65
Avg. deviation from averages	yes	--	--	--	±.010	±.015	±.016	±.019
Clear air	yes	1.00	(1)	4	1.008	1.001	0.985	1.020
" "	no	--	(1)	4	0.999	0.990	0.984	1.002
Plexiglass #1	yes	0.925	---	--	---	---	---	---
Plexiglass #2	yes	---	0.903	4	0.941	0.970	0.992	0.927
Glass	yes	0.861	0.858	3	0.863	0.856	0.839	0.873
"	no	0.891	0.858	1	**	~.875	~.87	~.88
Insect screen#1	yes	0.672	0.604	3	0.644	0.626	0.611	0.646
50% screen	yes	0.573	0.486	3	0.528	0.517	0.508	0.543
" "	no	0.685	0.486	1	**	**	0.506	0.566
30% screen	yes	0.409	0.192	3	0.324	0.292	0.277	0.327
" "	no	0.521	0.192	1	**	**	0.264	0.303
White paint	yes	0.247	(0).	4	0.274	0.143	0.118	0.156
" "	no	--	(0)	1	**	**	0.078	0.164
Black felt	yes	0.121	(0)	3	0.071	0.064	0.061	0.077
" "	no	--	(0)	1	**	0.136i	0.103i	0.082

* V_f was measured from avg. return during indicated time interval (Δt) after target.
V_n was measured from avg. return during 0.1 - 0.4 μsec before target.

** Oscillograms off scale or not yet settled.

× = Unmodified lidar (1971, ref. 1)
△ = Recent meas., Δt = .25 - .55 μs
o = Recent meas., Δt = .65 - .9 μs
□ = Recent meas., Δt = .9 - 1.9 μs

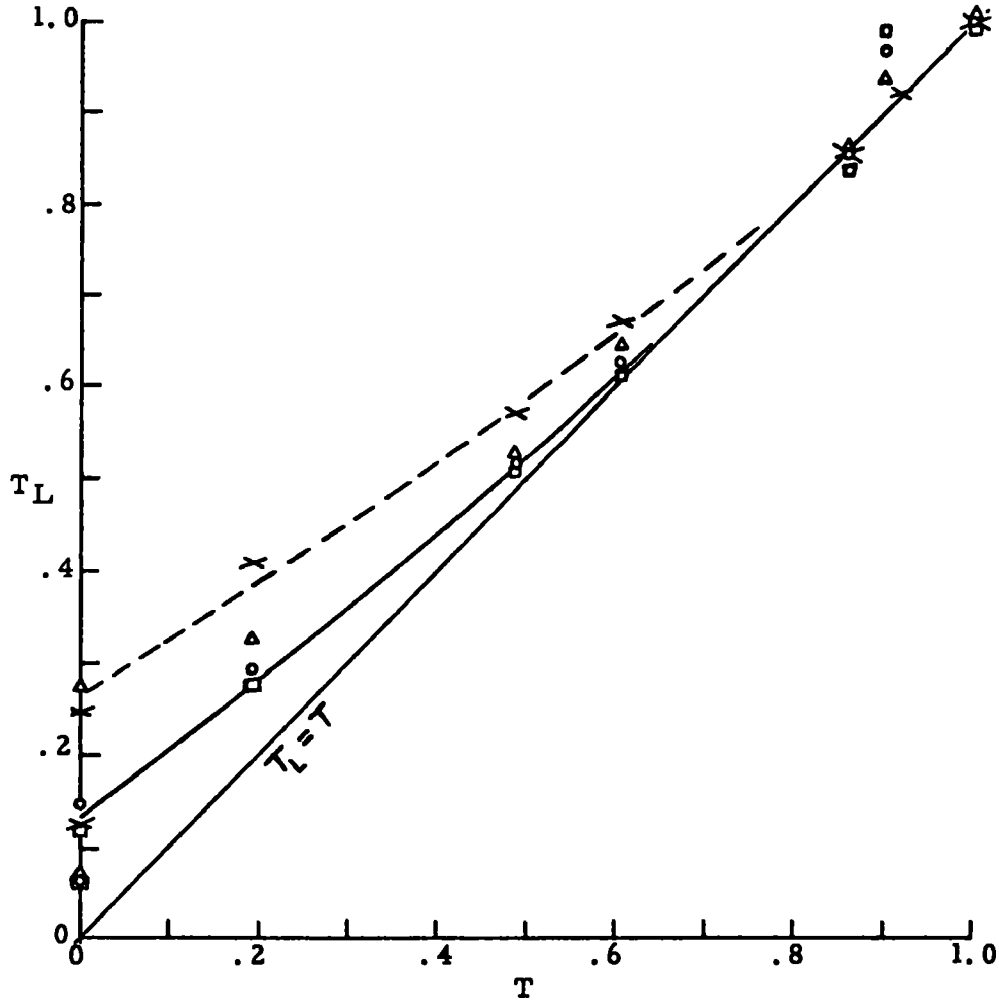

Figure 5.1 Averaged lidar-determined target transmittance (T_L) vs. laboratory-determined target transmittance (T). Only off-gated results are plotted. At T = 0, the upper point of each pair is the white target result and the lower point of each pair is the black target result. The upper solid curve is for the recent T_L results with Δt = 0.65 - 1.9 μs (o and □), while the dashed curve applies to the unmodified lidar results (×).

Figure 5.2 contains some sample oscillograms of off-gating lidar returns obtained during the recent test target measurements. Figure 5.2a shows a clear air gated lidar shot taken through the empty target holder during a period of relatively non-uniform atmospheric scattering. By contrast, Figure 4.4a shows relatively uniform atmospheric scattering as observed during a similar lidar shot through the empty target holder and taken only two minutes after the shot of Figure 5.2a. The remaining oscillograms of Figure 4.2 show sample oscillograms of similar lidar test shots taken through some of the targets listed in Tables 5.1 and 5.2.

One comment to be made about the recent test target results is that 3 out of the 4 Plexiglass oscillograms showed a far side (of target) return which increased with range. These same three lidar shots all hit the Plexiglass sheet at about the same spot (center), while the one, more normal, type shot had the laser beam moved to an off-center location. These three abnormal lidar returns (see Figure 5.2d for example) may be due to a lensing effect which is discussed in reference 1. For the above reasons, we discount the Plexiglass results in arriving at subsequent conclusions.

Another observation is that the one non-gated glass target oscillogram shows large near range variations in atmospheric scattering and thus in V_n. This made the corresponding transmittance results only approximate, as indicated in Table 5.2.

Although far fewer non-gated than gated lidar shots were made in the recent series of target measurements (Table 5.2), the non-gated results are generally comparable to the gated results. However, the gated results have the advantage of being valid at Δt smaller (V_f closer to the semi-reflecting target) than do the non-gated results. The non-gated shots yielded longer PMT plus circuit recovery times which usually limited V_f measurements to $\Delta t \geq 0.9$ microsecond.

A comparison of the recent non-Plexiglass gated lidar results (Table 5.2 and Figure 5.1) with the recent laboratory transmittance values show the most consistent agreement to be from $\Delta t = 0.65 - 1.9\ \mu s$. For the relatively transparent low reflectance targets, the $\Delta t = 0.25 - 0.55\ \mu s$ results are also very good, but they get worse as transparency decreases and reflectance (and thus PMT afterpulsing) increases. Thus, we find that, in general, we obtain the best transmittance results when measuring V_f with $\Delta t = 0.65 - 1.9\ \mu s$ and the PMT gated.

Now, a comparison of the recent gated $\Delta t = 0.65 - 1.9\ \mu s$ transmittance results with the 1971 lidar results (Table 5.2 and Figure 5.1 excluding Plexiglass) shows the modified lidar system to give about as good results at $T_L \geq 0.85$, and much better than the original system at $T_L = < 0.85$.

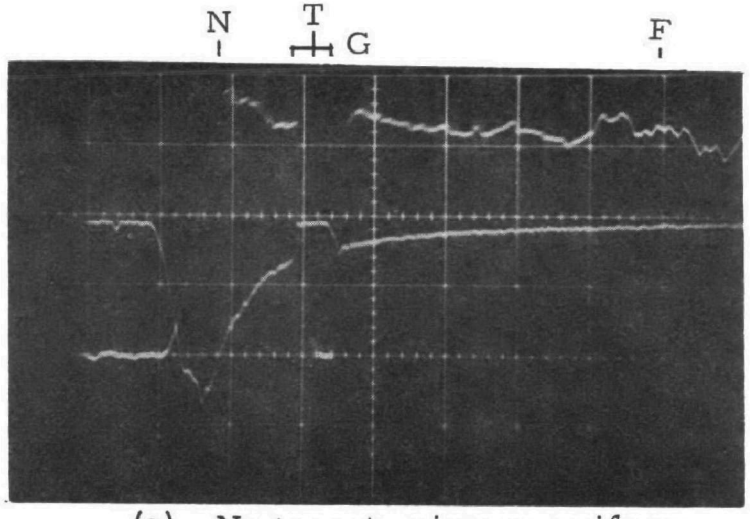

(a) No target, air non-uniform

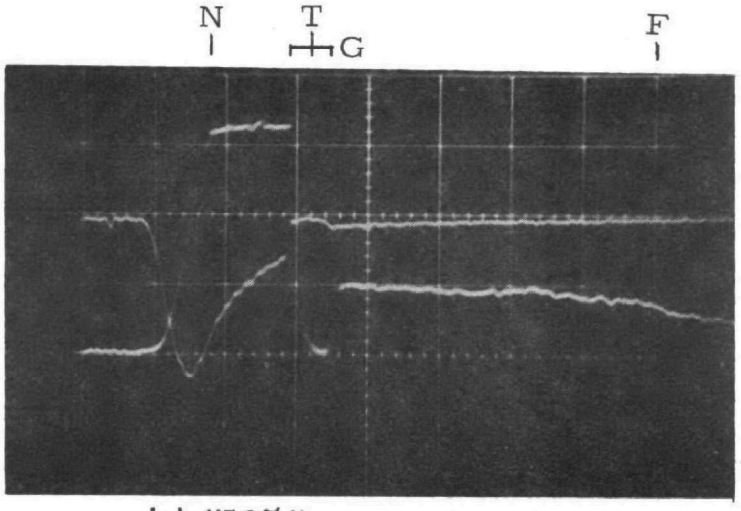

(c) "50%" screen target

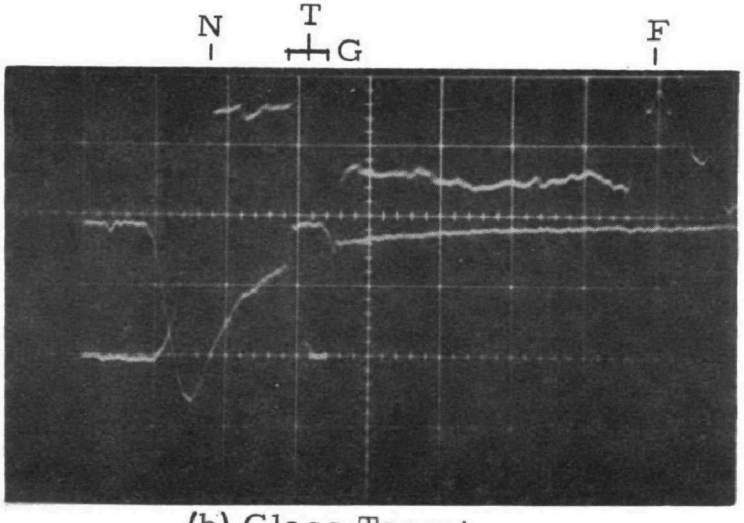

(b) Glass Target

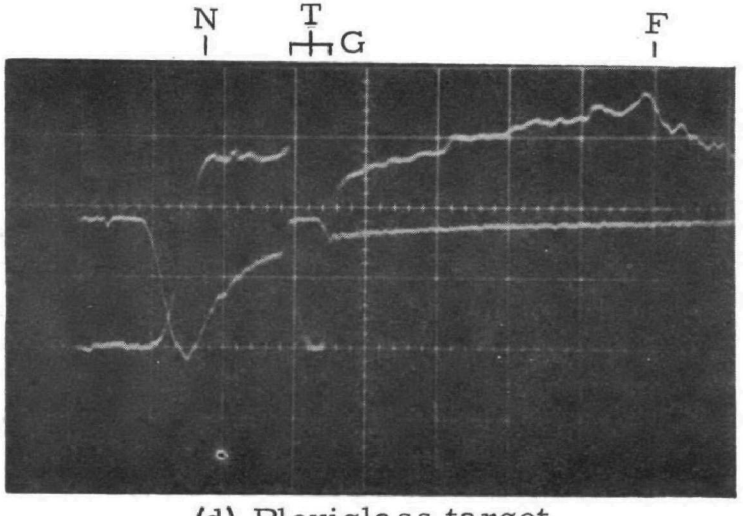

(d) Plexiglass target

Figure 5.2 Double beam oscillograms showing sample lidar returns during test target measurements while using the new PMT and time-squared amplifier (TSA). Each oscillogram is externally triggered by the laser monitor (not shown), and has a sweep speed of 500 ns/cm. In all cases, the negative-going lower trace (at 1 V/cm) is PMT input to the TSA, while the positive-going upper trace (at 0.1 V/cm) is TSA output with TSA gain at 5X. Off-gating intervals (all 260 ns) are indicated by G, target holder position by T, and the near and far limits of range correction by N and F, respectively.

In conclusion, it thus far appears that (1) the modified lidar system gives better results overall than the original lidar system; (2) the modified lidar system gives its best results when used (a) gated, (b) measuring V_n as close to targets as possible, and (c) measuring V_f with $\Delta t = 0.6 - 2\mu$ sec after the target; and (3) when used as suggested, the modified lidar system transmittance (T_L) results (a) are precise to $\pm$ 0.015 average, (b) are accurate to $\pm$ 0.02 average at $T > 0.5$, and (c) are too large at $T < 0.5$.

These results are to be compared (see Figure 5.1) with the pre-modification accuracies[1] of + .09, -0 at $T > 0.50$, and more severely too large at $T < 0.5$.

6. OPERATING INSTRUCTIONS FOR LIDAR MODIFICATIONS

The originally issued instruction manual[3] still applies to the use of this lidar system except where modifications have been made as discussed in this report. Thus all of Table 2. 1 and nearly all of Figure 2. 2 of this report still apply (Table 1. 1 and Figure 1. 4 of reference 3). A detailed discussion of the new detection system characteristics and circuitry is covered in Section 3 of this report, while Section 4 similarly covers the range-correcting time-squared amplifier (TSA). Thus this Section 6 is concerned with how the lidar modifications influence the overall system hookup, and necessary or potential circuit adjustments in the detection system and TSA.

Figure 6. 1 shows a detailed block diagram of an externally triggered method for simultaneously recording the lidar data in both direct and range-corrected forms. It should also be noted that Figure 6. 1 shows slight modifications in the laser energy monitor/trigger system as compared with Figure 1. 9 of reference 3. Except for changing the energy monitor calibration curve, this laser monitor modification results in no alteration of instructions[3] for its use.

6. 1 Use of the Modified Lidar Receiver System

6. 1. 1 Photomultiplier Tube Operating Voltage Selection

As discussed in Section 3. 3. 4 there is a space charge linearity limit on photomultiplier tube (PMT) output current (and thus on voltage across the 93 ohm load) that depends on the PMT overall operating voltage, increasing as the voltage is increased, but increasing far slower than PMT gain (Fig. 3. 2) with respect to applied voltage. Thus, it is possible to select a PMT applied voltage that will produce a non-linear near range signal. In the extreme it may be possible to produce a sufficiently large, non-linear, near range signal that the dynode capacitors are depleted and not only the near range but all greater range signals will be non-linear.

The optimum applied voltage is that which yields a near range signal maximum equal to or slightly larger than the space charge linearity limit of 2 to 3 volts (93 ohm load) since this will allow maximum system range. This applied high voltage is determined empirically by observing the lidar maximum signal and adjusting the PMT voltage until the condition is met. The voltage required will vary day to day depending on the ambient aerosol scattering, but a good trial value is 1700 volts.

For any applied voltage, the PMT dc output should be < 5 percent of the divider chain current obtained by dividing the applied tube voltage by the divider chain resistance of about 1. 16 megohms. If it is not, tube operation will no longer be linear at any range. For 1500 volts applied, the dc output thus should be $< 65\ \mu a$ ($< .006$ V with a 93 ohm load. The use of larger applied PMT potentials would result in proportionately larger dc output limits.

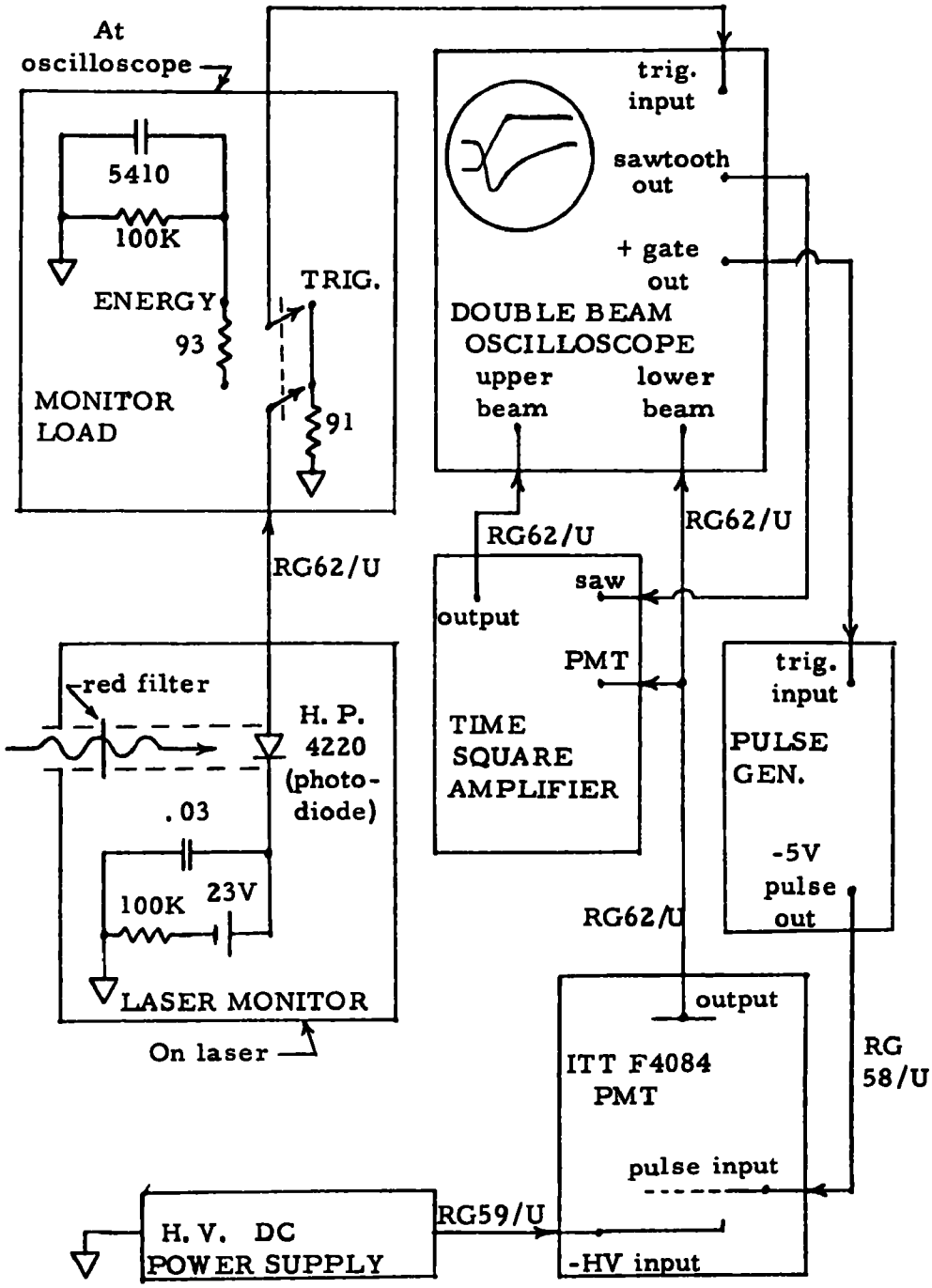

Figure 6. 1 Lidar data recording system with double beam oscilloscope presentation of photomultiplier tube (PMT) output, both direct and range-corrected via the time-squared amplifier. This figure also shows the laser trigger/energy monitor system in the trigger mode.

For the reasons discussed in Section 3.2, the total potential applied to the PMT should not exceed 2500 volts. In the event that the PMT is operated outside of the 1500 - 2000 volt range (see Section 3.3.2), the applied gating pulse or PMT grid, and perhaps the PMT focus electrodes, should be re-adjusted for the new voltage range as described in Section 6.2 below.

6.1.2 Obtaining the Proper Off-Gating Pulse Position

Before transmittance measurements can be made, it is necessary to establish the correct position for the gating pulse. This is done by using the lidar system as a rangefinder. The lidar is aimed at the smoke plume (or the top of the stack if it is diffusely reflecting) and is fired with the oscilloscope recording the PMT output at 10 V/cm. For this purpose, use a simple 93 ohm load at the oscilloscope or set the TSA "Mode" switch on direct ("Dir", see Fig. 4.1). The oscilloscope sweep should initially be set at 0.5 μ sec/cm (ranges of 2500 ft. or less) and should be decreased if no sharp spike return is visible. The return from the plume or stack will generally produce a saturated PMT output of from 10 to 20 volts which will not faithfully reproduce the width of the plume, but will give a sufficiently good range value so that by comparing the ranging oscillogram with the variable position of the -5 volt gating pulse, the gating position can be set.

The -5.0 volt gate position and gate width can most easily be checked and adjusted between lidar shots while using the same 93 ohm load or TSA direct mode setting as used above for determining target range. However, now the oscilloscope sensitivity should be set at 0.01 or 0.02 V/cm and the oscilloscope trigger should be set in the automatic mode. In this mode the oscilloscope triggers at a sweep frequency of 60 Hz. This provides a gate out which triggers the pulse generator providing a gating pulse to the 50 ohm load in the PMT housing. The derivative of the gating pulse is weakly coupled to the anode circuit and thus is available as a negative going and a positive going set of spikes defining the gating pulse position and duration. It is recommended that an off-gating pulse width of at least 200 nsec be used because of range uncertainties combined with the non-rectangular temporal shape of the laser pulse and appreciable thickness of the smoke plume.

6.1.3 Taking Transmittance Data

As detailed in Section 4 and indicated in Figure 6.1, the range-correcting time-squared amplifier (TSA) must receive an appropriately timed linear ramp. This is accomplished by connecting the lidar oscilloscope (Tektronix Model 551) 0 to + 150 V "sawtooth out" to the TSA "saw" (sawtooth input) BNC connector (Figure 4.1). Also, the RG62/U coaxial cable from the PMT anode "output" (Figure 3.1) is connected to the TSA "PMT" (PMT input) BNC connector without the use of any external load resistor. Finally, a short length of RG62/U coaxial cable is run from the TSA "output" BNC connector to one of

the oscilloscope vertical inputs which is normally set at 0.1 or 0.2 V/cm sensitivity. The oscilloscope other vertical input may be connected to the TSA "PMT" input via a BNC Tee connector plus a short length of RG62/U cable as shown in Figure 6.1. When the oscilloscope is triggered externally as shown in Figure 6.1, this general method yields oscillograms similar to those shown in Figures 4.3, 4.4, and 5.2. To trigger in this manner, set the monitor on "trigger" and attach it to the oscilloscope "trigger input" with trigger settings being slope = "EXT +", Mode = "AC (LF reject)", stability = "preset", and level = slightly positive. An alternate display option is to connect the second oscilloscope vertical input to the laser energy monitor ("energy" setting) and trigger the oscilloscope internally.

Before the first lidar shot using the TSA, preset its controls as follows (see Figure 4.1): set "mode" switch to "XT^2", set "gain" to "5X" and set "signal flatness" to 7.0 (range = 1 to 11). Although the TSA will operate almost immediately after being turned on, the screwdriver lockable "zero" adjustment has been pre-set to an optimum value for the TSA after it has warmed up for at least 10 or 15 minutes. The TSA zero signal level noise output with grounded "PMT" input is about 8 mV pp (about 1.5 mV rms), with the zero signal flatness being influenced by the "zero" setting as discussed in Section 6.3. The screwdriver lockable "far limit" adjustment has been pre-set for a far limit of range compensation at 0.9 scope sweep from time zero when the sweep is set at 500 ns/cm and the TSA "signal flatness" is set at 7.0. This 0.9 sweep far limit is slightly altered by other settings for signal flatness and scope sweep. See Section 6.3 for checking and readjusting the "far limit". (For the lidar oscillograms shown in Figures 4.3, 4.4, and 5.2, the TSA "far limit" (F) had been set closer to 0.8 scope sweep).

A sample lidar shot can now be made into clear air alongside the plume target and the TSA "signal flatness" adjusted if necessary. Figure 4.3 shows examples of lidar returns with "signal flatness" correctly adjusted and also at the extremes of adjustability. As can also be seen from the oscillograms of Figure 4.3, the near range limit (N) for range compensation is determined by that range (time) at which the product of direct PMT volts times TSA "gain" setting drops to a value of 10. Thus the near range limit (N) can be varied by an appropriate combination of choices of (a) TSA gain (3X, 5X, or 10X), (b) PMT high voltage and thus PMT gain (see Fig. 3.2), and (c) lidar laser output energy. When selecting the final PMT high voltage and TSA "gain", do not exceed the PMT linearity limits at the near range point N or the PMT high voltage limits as indicated in Section 6.1.1 and detailed in Section 3.3.

Because there is a surplus of TSA and PMT gain combinations available, the laser output need never be pushed to even 0.5 joule/pulse. In fact, operating the laser at outputs of only 0.2-0.4 joule/shot will contribute to longer flashlamp life, longer life of optical components within the laser cavity, and especially will result in somewhat narrower laser outputs ($\leq$ 30 ns FWHH) than

might be obtained if the laser is driven hard. A wide or multiple laser output might require longer off-gating and a resulting greater requirement of atmospheric uniformity for transmittance measurements.

With all of the lidar receiver adjustments now completed, the actual transmittance-measuring lidar shots are made through the plume of interest. If the lidar return trace shows ringing and slow recovery after the plume (see Fig. 4. 4c) or is driven to a large off scale value at the plume (rather than dropping to zero), then the off-gating pulse starts too late or ends too soon and must be adjusted.

6. 2 Internal Description and Adjustment of Detection System

It is not anticipated that the following procedures will be required, but they are included in the event that the photomultiplier tube (PMT) must be replaced or it is desired to change its operating voltage outisde of the 1500-2000 volts range while off-gating. As delivered, all PMT adjustments were made at an applied potential of 1750 volts while using -5. 0 volt off-gating pulses.

As indicated in Figure 3. 1, this ITT type F4084 PMT fits into a 15 hole socket which handles all tube connections except for the photocathode and internal control grid, both of which have flying leads (external wires) running from the cathode end of the tube. Also, the PMT anode is internally connected to a General Radio type 874-B coaxial connector which projects from the center of the PMT base. The anode output is then directly conducted to the PMT housing "output" BNC connector via a semi-flexible lead which is press-fitted into the 874B connector. In addition, the PMT housing has an inner cylindrical "shield" which is held at cathode potential via a flying lead soldered to a lug at the cathode (open) end of the shield tube. This inner cylindrical shield is positioned and insulated from the outer cylindrical housing body and other grounded housing parts by a specially shaped Teflon spacer ring at each end. Also, because the PMT fits fairly loosely in its socket, the PMT is braced near its cathode end with a foam rubber plus Teflon tape spacer between the PMT and the rigidly held shield.

To remove the PMT, first disconnect all external cables to the housing and then remove the PMT housing from the lidar receiver at the housing flange (3 Phillips head screws). Next, all three flying leads must be unsoldered at points "K", "IG", and "Sh" from the divider/gating circuit (see Figure 3. 1) which is located in the gray rectangular box at the base end of the PMT housing. Do not attempt to remove the flying leads from the PMT. Also, the press-fit anode wire must be pulled from the 874B connector at the center of the tube base. This is also accessed from the gray box at the base end of the PMT housing. Once these disconnections have been made within the divider/gating circuit box, the black outer (ground) cylindrical tube and inner cylindrical shield can be pulled off the circuit box flange after unscrewing the three 6-32 Allen head bolts spaced around the circuit box end of the cylindrical housing. This exposes the PMT which can then be removed. If it is only desired to expose the PMT but not to remove it, then only the shield flying lead (white) need be disconnected

at the shield or at "Sh", Fig. 3. 1. The inner shield and outer tube are then removed as above while pressing lightly on the PMT face to make sure it does not pull out with the shield tube.

Any time the PMT housing is removed from the lidar receiving system or even if the entire detection system is removed including the interference filter section (such as for a lidar system alignment check[3]), first turn off the PMT high voltage power supply and disconnect all external cables from the PMT base. This is especially important for the high voltage connector, as the PMT could be damaged by exposure to excessive light if the high voltage were still on.

All PMT focus electrode and internal grid adjustment potentiometers ("pots") are located inside of the gray rectangular box at the base end of the PMT housing. Since all of these adjustments must be made with the back cover of the box removed and the PMT operating at the desired high voltage, care must be taken to keep fingers and metal tools away, and to make all adjustments only with a nonconducting screwdriver. Also, avoid directing bright light into the open circuit box because of small light leaks from the circuit section to the PMT section. Normal indoor room lighting is OK.

To adjust the focus electrode pots or internal control grid pot (Fig. 3. 1), it is also necessary to provide a suitably weak dc light source which does not overdrive the PMT (see Section 3. 3. 4). This could be accomplished through the entire detection system assembly which includes the interference filter. The focus electrodes can be adjusted at low PMT output currents as measured with an electrometer or by using a large value load resistor (10K - 100K) at the oscilloscope. Adjust the focus electrode pots for maximum PMT output in the order F1, F2, F3, F4 and then repeat (see Figure 3. 1). These pots are numbered 1, 2, 3, and 4, and are accessible from the open back of the divider/ gating circuit box as indicated above.

The PMT control grid adjustment pot has a brown insulating extension attached to its shaft, and a piece of transparent tape which locks the pot to its present setting. To optimize the PMT off-gating for a different applied high voltage, it is first necessary to remove the locking tape. Be sure the high voltage is turned off before removing or replacing the tape. Now the dc light source must be adjustable and turned up to yield a measurable dc anode output signal across a 93 ohm load at the oscilloscope while at the same time always keeping the anode current less than 0. 1 of the divider circuit current. This is accomplished by setting the scope sensitivity at 0. 005 V/cm, and always limiting the dc voltage drop from the PMT anode output across the 93 ohm load to no more than 2 cm (10 mV) as shown in Figure 3. 3. While the -5. 0 volt off-gating pulse is repeatedly applied to the PMT housing "pulse input", the control grid pot is adjusted to give a symmetric anode output gating response such as is shown in Figure 3. 3a.

An alternate method for adjusting off-gate symmetry which avoids opening the divider/gating circuit box and changing the grid adjustment pot, is to change the -5 volt gating pulse to a different voltage which again results in symmetric off-gating. The use of this simpler method may result in slight changes in gating on/off ratio or in gating response time.

6.3 Time-Squared Amplifier Adjustments

The most routine front panel adjustments have already been discussed in Section 6.1.3. Except for the front panel "zero" setting, the other adjustments will seldom if ever need to be performed. However, the procedures are included here in the event that it is desired to change the time-squared amplifier (TSA) operating characteristics, or if TSA components need to be replaced.

In preparation for the taking of lidar data, the TSA front panel "far limit" control may be checked and altered if desired. On delivery, this lockable screwdriver adjustment was pre-set for 9 cm of oscilloscope sweep with the sweep set for 500 ns/cm and the TSA "signal flatness" set at 7.0. The far limit for range compensation is readily observed by temporarily applying -0.1 to -0.5 volts dc to the TSA "PMT" input (TSA mode = XT^2) and self-triggering the oscilloscope by setting it in the "automatic" mode. The time-squared ramp will then be presented to the scope via the TSA "output" connector, with the t^2 ramp leveling off at the far limit for t^2 range correction (points F of Figure 6.2a). As seen from Figure 6.2a, the far limit for range correction varies somewhat with the "signal flatness" (SF) setting. It also varies somewhat with the scope sweep speed. The upper trace of Figure 6.2a shows the TSA far limit setting as delivered. One convenient source for the dc voltage input could be a 1.5 or 3 volt dry cell in series with a 1000 ohm resistor.

It may occasionally be desirable to check and adjust the TSA output zero signal shape. This is easily accomplished by looking at the TSA output while (a) having the PMT on and the lidar receiving system looking at its target (but no laser shot), (b) setting the oscilloscope at its lidar-use sweep speed (usually 500 ns/cm), (c) automatically triggering the scope at its internal 60 Hz rate, and (d) increasing the scope sensitivity to about 0.01 V/cm. The top three traces of Figure 6.2b show typical zero signal returns with no signal at the TSA "PMT" input. The TSA front panel screwdriver adjustable "zero" setting permits optimization of the zero signal shape (flatness). This shape will stabilize as the TSA becomes fully warmed up.

Analog multiplier M1 (see Figure 4.1) has a zero adjustment vernier pot located inside the circuit box and accessed by removing the top cover. The system operation is so insensitive to this adjustment that it should never need to be corrected. However if the adjustment is checked or the M1 unit changed, that pot should be adjusted (after full warm up) so test point T6 reads 0mV when test point T5 is grounded (first disconnect the sawtooth input from the oscilloscope).

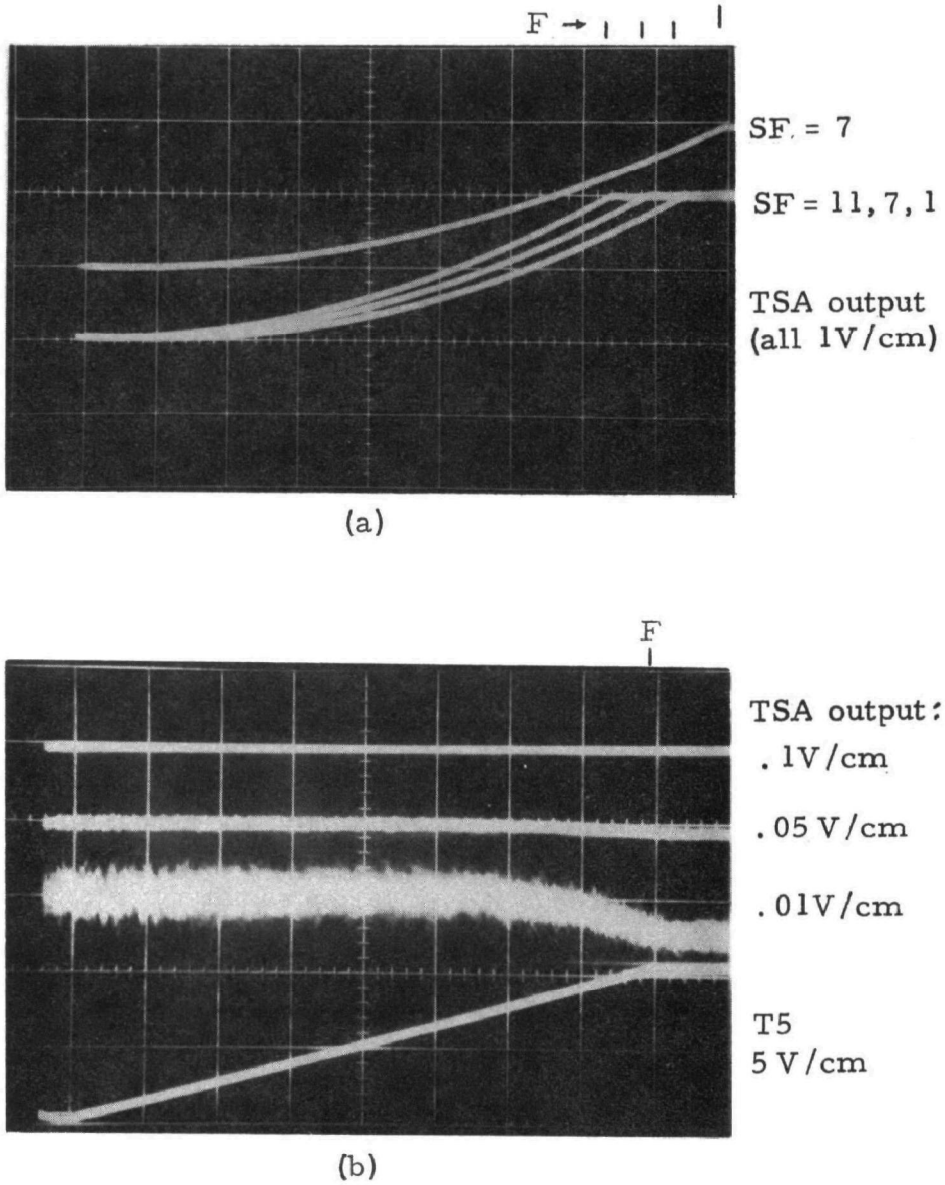

Figure 6.2 Oscillograms showing some time - squared amplifier (TSA) adjustments and characteristics with TSA "gain" at 5X. All oscillogram sweep speeds are 500 ns/cm. In all cases, the range correction ends at point F. Figure 6.2a shows TSA output (all at 1V/cm) with -0.4V dc at the "PMT" input and two "far limit" settings. The lower group of three superposed traces all have the same "far limit" setting but have the "signal flatness" (SF) varied (left to right) from 11 to 7 to 1. The top three traces of Figure 6.2b show the TSA output shape and noise when the "PMT" input is grounded. This zero signal output shape can be varied and optimized with the "zero" control. The lowest trace of Figure 6.2b shows the simultaneous ramp signal at test point T5 of the TSA (see Fig. 4.1).

The gain-control feedback capacitors C1, C2, and C3 of the TSA operational amplifier A521 (see Figure 4. 1) have already been adjusted for optimum A521 response as described in Section 4. 2 and shown in Figure 4. 2a. These capacitors should never need re-adjustment unless the operational amplifier is replaced or the feedback system altered. If this re-adjustment procedure should ever be necessary, apply a fast response square wave of -0. 1 to -0. 5 volts to the TSA "PMT" input and observe the amplifier output at test point T3 with an oscilloscope probe. Then adjust the variable capacitors C1, C2, and C3 (they are numbered) for optimum operational amplifier performance at gain settings of 3X, 5X, and 10X, respectively. These capacitors and T3 are accessible by removing the TSA box top cover.

7. SUMMARY AND CONCLUSIONS

This study was intended to eliminate the dominant source of error in the remote measurement of smoke-stack plumes using lidar, and to improve the data presentation of the lidar transmittance measurement.

The use of a special grid-controlled photomultiplier tube and off-gating system has resulted in a large reduction of photomultiplier tube afterpulsing which has been the principal problem limiting the accuracy of plume transmittance measurements.

A range-correcting time-squared amplifier has also been developed which permits much faster and more convenient data reduction than formerly possible.

The above two developments have been adapted to the existing van-mounted EPA lidar system, and the overall system accuracy has been evaluated using both opaque and semi-transparent targets of known transmittance (T). These test results show the lidar system to yield lidar transmittances (T_L) which (a) are precise to $\pm$ 0.015 average, (b) are accurate to $\pm$ 0.02 average for $T > 0.5$, and (c) are too large at $T < 0.5$ (for example, now $\overline{T}_L = 0.52$ at $T = 0.50$, and $T_L = 0.28$ at $T = 0.20$). These results are to be compared with the pre-modification accuracies of + .09, -0 at $T > 0.50$, and more severely too large at $T < 0.5$ (for example, formerly $T_L = 0.59$ at $T = 0.50$, and $T_L = 0.40$ at $T = 0.20$).

8. REFERENCES

1. C. S. Cook and G. W. Bethke, "Design, Construction and Evaluation of a Mobile Lidar System for the Remote Measurement of Smoke Plume Opacity", Final Report, EEI Research Project RP39 and EPA Contract No. 68-02-0093, December 21, 1971.

2. C. S. Cook, G. W. Bethke, and W. D. Conner, "Remote Measurement of Smoke Plume Transmittance Using Lidar", Appl. Opt. 11, 1742 (1972).

3. "Mobile Lidar System Operating Manual", EEI Research Project RP39 and EPA Contract No. 68-02-0093, January 1972.

BIBLIOGRAPHIC DATA SHEET	1. Report No. EPA-650/2-73-040	2.	3. Recipient's Accession No.
4. Title and Subtitle Development of Range Squared and Off-Gating Modifications for a Lidar System.			5. Report Date (preparation) September 1973 6.
7. Author(s) GEORGE W. BETHKE			8. Performing Organization Rept. No. NONE
9. Performing Organization Name and Address General Electric Company Space Division - Space Sciences Laboratory P.O. Box 8555 -- Philadelphia, Pennsylvania 19101			10. Project/Task/Work Unit No. 11. Contract/Grant No. 68-02-0570
12 Sponsoring Organization Name and Address Chemistry and Physics Laboratory National Environmental Research Center Research Triangle Park, North Carolina 27711			13. Type of Report & Period Covered Final Report 6/27/72 to 9/5/73 14.

15. Supplementary Notes

16. Abstracts

This study was intended to eliminate the dominant source of error in the remote measurement of smoke-stack plumes using lidar, and to improve the data presentation of the lidar transmittance measurement. The use of a special grid-controlled photomultiplier tube and off-gating system has resulted in a large reduction of photomultiplier tube afterpulsing which has been the principal problem limiting the accuracy of plume transmittance measurements. A range-correcting time-squared amplifier has also been developed which permits much faster and more convenient data reduction than formerly possible. The above two developments have been adapted to an existing van-mounted EPA lidar system; and the improved overall system accuracy has been evaluated using both opaque and semi-transparent targets of known transmittance.

17. Key Words and Document Analysis. 17a. Descriptors

* Air Pollution; Smoke
* Transmittance; Opacity
* Optical radar; Optical detection
* Remote sensing; detection
* Photomultiplier tubes
* Range gating
* Data reduction, data processing
* Data processing; data reduction, data acquisition

17b. Identifiers/Open-Ended Terms

Remote measurement of plume transmittance
Photomultiplier tube gating
Lidar range correction
Time squared amplifier

17c. COSATI Field/Group 14B, 9E

18. Availability Statement	19. Security Class (This Report) UNCLASSIFIED	21. No. of Pages 51
	20. Security Class (This Page UNCLASSIFIED	22. Price